IOP PUBLISHING NONLINEARITY

Nonlinearity **20** (2007) 2425–2452 doi:10.1088/0951-7715/20/10/009

Why is a shock not a caustic? The higher-order Stokes phenomenon and smoothed shock formation

S J Chapman[1], **C J Howls**[2,5], **J R King**[3] **and A B Olde Daalhuis**[4]

[1] Mathematical Institute, University of Oxford, 24–29 St Giles, Oxford, OX1 3LB, UK
[2] School of Mathematics, University of Southampton, Highfield, Southampton, SO17 1BJ, UK
[3] School of Mathematical Sciences, University of Nottingham, University Park, Nottingham, NG7 2RD, UK
[4] School of Mathematics, The University of Edinburgh, Kings Buildings, Mayfield Road, Edinburgh, EH9 3JZ, UK

Received 27 March 2007, in final form 14 August 2007
Published 12 September 2007
Online at stacks.iop.org/Non/20/2425

Recommended by L Ryzhik

Abstract

The formation of shocks in waves of advance in nonlinear partial differential equations is a well-explored problem and has been studied using many different techniques. In this paper we demonstrate how an exponential-asymptotic approach can be used to completely characterize the shock formation in a nonlinear partial differential equation and so resolve an apparent paradox concerning the asymptotic modelling of shock formation. In so doing, we find that the recently discovered higher-order Stokes phenomenon plays a significant, previously unrealized, role in the asymptotic analysis of shocks. For the purposes of clarity, Burgers' equation is used as a pedagogical example, but the techniques illustrated are more generally applicable.

Mathematics Subject Classification: 34M40, 34M60, 34M37, 34E-xx, 35L67, 35L70, 74J30, 74J40

1. Introduction

The aim of the present paper is to further our understanding of exponential-asymptotic techniques in the area of nonlinear partial differential equations. A natural starting place is to use such techniques to solve an equation, the behaviour of whose solutions is already very well known. To that end we shall study the pedagogical example of Burgers' equation

[5] Author to whom any correspondence should be addressed.

and consider the role of beyond-all-orders asymptotic effects in shock formation. However, we shall see that, even for such a well-studied problem, the use of exponential asymptotics throws up surprising and rather generic phenomena.

There is a vast toolbox of existing asymptotic techniques to attack and interpret shock formation, one of the most obvious being matched expansions. At the outset, we stress that we are not proposing that an exponential-asymptotic approach should replace that of matched asymptotics in shock situations. However there are outstanding subtle issues associated with the asymptotic modelling of shock formation that can nevertheless be resolved and explained by taking a beyond-all-orders approach.

For example, often the necessity of matched asymptotic expansions is indicated through a sudden blow up of a naive expansion, which indicates how a rescaling should be made. However, for some problems there is nothing in the behaviour of the expansions *per se* to suggest that a shock is imminent. The shock has to be supposed to exist to remove a difficulty of multivaluedness of a solution, and then the matched asymptotic solution is shown to be self-consistent. By contrast, an exponential asymptotic automatically detects the shock and provides a transitional approximation across it. Indeed, whenever one asymptotic expansion fails to predict an approaching breakdown it is often a sign that there is an exponentially small correction term that is about to become of order one (that is, we are near an anti-Stokes line). At the most obvious level, a beyond-all-orders approach shows how these exponentially small correction terms naturally arise in Burgers' equation without the need for matching, and how it is these that are ultimately responsible for shock formation and propagation. These corrections are related to the existence of complex singularities in the vicinity of the shock region. The link between the size of exponential-asymptotic terms and formation of singularities was shown before, in [7].

Moreover there is a second, extremely subtle, but far reaching reason for considering exponentially small terms in more detail. At first sight, a reader familiar with a matched asymptotic approach to shock formation might consider the idea that the growth of exponentially small terms (of WKBJ-type) to form a shock unsurprising and entirely unoriginal. However, this apparent familiarity masks the existence of a significant paradox in the underlying exponential-asymptotic process, associated with the observation that exponentially prefactored expansions of WKBJ-type exchange dominance in two ways. First, the exchange may take place as an anti-Stokes line, where the differences in the real parts of their exponents vanish, is crossed in the relevant parameter space. Secondly, the exchange may take place at locations where the exponents themselves are identical. The latter occurrence is often associated with turning points in one (complex) dimension or, in higher dimensions, at caustics. At caustics the non-uniform asymptotic series cease to be valid, as is often indicated by the singular nature of individual terms in the expansion. (Traditional examples of this are the divergence of the terms in the large $|z|$ asymptotic expansions of the Airy function $\mathrm{Ai}(z)$ at $z = 0$ or the Pearcey function on the cusp caustic, in optical situations [2], or the breakdown of local asymptotics in the wake of the Kelvin ship wave.) Hence, if a non-oscillatory shock is viewed as an exchange of exponential dominance at an isolated (moving) position on the real axis, asymptotically it is necessary to explain the absence of a catastrophic (caustic-related) breakdown in the expansion at smoothed shock, i.e. why is a shock not a caustic?

Here we show that the recently discovered concept of the higher-order Stokes phenomenon [5,6,10] plays a crucial role in resolving this paradox and can be regarded as being instrumental to the formation of the shock wave. This naturally leads to the identification of the shock as a 'virtual caustic' [1]. Consequently, the higher-order Stokes phenomenon and concepts of virtual caustics are fundamental exponential-asymptotic properties that can be seen to underpin the success of a matched asymptotic approach. Although our analysis is for a particularly

simple set of initial data in a simple problem, the techniques we use are much more generally applicable [11].

In section 2 we examine shock formation in the pedagogical example of Burger's equation and recall the determination of the location of the (smoothed) shock via a matched asymptotic approach. This establishes the notation and the basis for the rest of the paper. We embed the problem in complex space in section 3 and introduce the role of both real and complex caustics of the underlying rays. In section 2 we derive the template of the expansions used in the exponential-asymptotic solution of the problem and, for clarity, give an indication of the final asymptotic expressions. The details of the calculation of the exponents and important coefficients in these expansions are found in section 5. Using a Borel-plane approach, it is possible (section 6) to examine the beyond-all-orders properties of the solution on a path of analytic continuation from regions of space ahead of the shock, that passes through the shock. The natural genesis of the shock from exponential asymptotics is hence explained in section 6 together with the resolution of the apparent paradox of the absence of a catastrophic failure at the shock. In addition, the crucial role of the higher-order Stokes phenomenon in the uniformity of the process is explained.

Previous exponential-asymptotic studies of shock formation, for example, [12, 20] have been concerned with the role of exponentially small terms governing shock location in exponentially slow movement of the shock on a finite domain. We shall not discuss such issues here. Other work [3, 4, 18, 19] concerns the study of the Riemann-sheet structure of the Burgers' problem, complex pole dynamics and condensation. The complex approach in this paper is related and complementary, but the use of the higher-order Stokes phenomenon here means that the present work goes significantly beyond such previous analyses.

2. Burgers' equation

We consider Burgers' equation [21]

$$u_t + uu_x = \epsilon u_{xx}, \tag{1}$$

where

$$x \in \mathbb{C}, \qquad t \geqslant 0, \qquad \epsilon \to 0^+. \tag{2}$$

For clarity, in order to set up the problem, we shall first review pedagogically the main issues associated with smoothed shock formation in such a system, namely the potential multivaluedness of the solution and its resolution by imposition of a shock through matched asymptotic expansions.

We choose not to use a Cole–Hopf approach that would lead to exact integral expressions. This is to emphasize that the ideas we suggest here do not depend on the existence of explicit, exact solutions or integrability of the governing partial differential equation (PDE). A parallel investigation using a Cole–Hopf approach may be found in [13]. Generalizations of our approach to other nonlinear shocks can be found in [11].

For clarity of exposition we choose the initial conditions

$$u(x, 0) = \frac{1}{1 + x^2}, \qquad \text{and} \quad u \to 0 \quad \text{as} \quad |x| \to \infty. \tag{3}$$

The approach we take should work for analytic initial data giving rise to three or more possible asymptotic contributions (in particular, the existence of poles at finite complex positions in the initial data is not significant): the following analysis would equally apply to initial data of the form $u(x, 0) = 4x^3 - x$, say, with few modifications.

In the first instance, we seek a formal solution of the form

$$u(x,t;\epsilon) \sim \sum_{r=0}^{\infty} a_r(x,t)\epsilon^r, \tag{4}$$

where $a_0(x,t)$ satisfies the inviscid Burgers' equation

$$\frac{\partial a_0}{\partial t} + a_0 \frac{\partial a_0}{\partial x} = 0, \qquad a_0(x,0) = \frac{1}{1+x^2}, \tag{5}$$

and for $r \geqslant 1$ the $a_r(x,t)$ satisfy

$$\frac{\partial a_r}{\partial t} + \sum_{s=0}^{r} a_{r-s} \frac{\partial a_s}{\partial x} = \frac{\partial^2 a_{r-1}}{\partial x^2}, \qquad a_r(x,0) = 0. \tag{6}$$

Solving (5) by the method of characteristics implies that a_0 is constant on the characteristic projections $\mathrm{d}x/\mathrm{d}t = a_0$. Thus the solution in parametric form is

$$x = \xi + \frac{t}{1+\xi^2},$$

where ξ is the (possibly complex) value of x at $t = 0$. This has three solutions for ξ, corresponding to three rays (characteristic projections) of (5) through each point (x,t); we label these values of ξ as x_0, x_1 and x_2, so that

$$a_0 = a_0(x_j) = \frac{1}{1+x_j^2}, \qquad j = 0, 1, 2. \tag{7}$$

on the rays

$$x = x_j + a_0(x_j)t, \qquad j = 0, 1, 2, \tag{8}$$

where, here and henceforth, we have abbreviated $a_0(x_j, 0)$ to $a_0(x_j)$. (Note that the $x_j(x,t)$ are the locations of the saddle-points in a steepest descent analysis of the Cole–Hopf representation of the solution.)

The families of rays generated by the x_j are tangential at caustics which simultaneously satisfy both (8) and

$$0 = 1 + \frac{\mathrm{d}a_0(x_j)}{\mathrm{d}x_j} t, \qquad j = 0, 1, 2. \tag{9}$$

For the chosen initial conditions, the caustics are given by

$$27t^2 - 4tx(9+x^2) + 4(1+x^2)^2 = 0. \tag{10}$$

Four branches emanate from the singular points of the initial data. Two branches emerge from $+i$, two from $-i$. Two of the branches intersect the real x-plane at the cusp point $(x_c, t_c) = (\sqrt{3}, 8/\sqrt{27})$, one from $+i$, one from $-i$. The remaining two branches recede away from the real x-plane into complex space as t increases. These latter two caustics will be discussed when we give the complete geometry of the Stokes surfaces of the problem below.

For the moment we focus on the two caustics that intersect at the real cusp point. These are shown in figure 1. These caustics separate the (x,t)-plane into two regions. On the 'outside' of the caustics there is one real ray through each point (i.e. only one of the solutions x_j is real); see figure 2. We label the starting point of this ray x_0. Dismissing the rays originating at complex values of x_j as unphysical, this gives the unique solution for a_0 as $a_0(x_0(x,t))$. On the other hand, on the 'inside' of the caustics all three rays are real and originate from $t = 0$ at x_0, x_1 and x_2, where we adopt for later use the convention that

$$x_1 < x_2 < x_0. \tag{11}$$

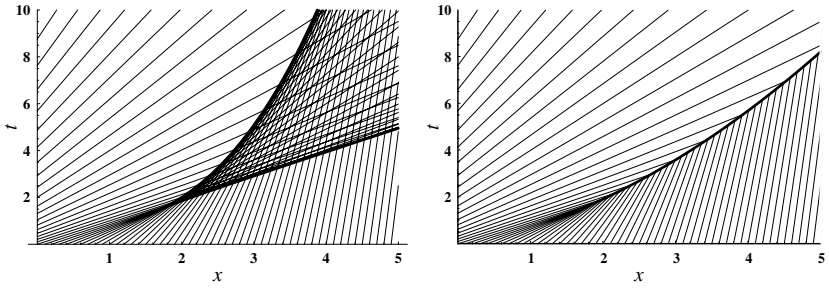

Figure 1. Rays, caustics and shocks for Burgers' equation with initial data (3) for $x, t \geqslant 0$. The bold lines denote the caustics (left) and the constructed shock position (right).

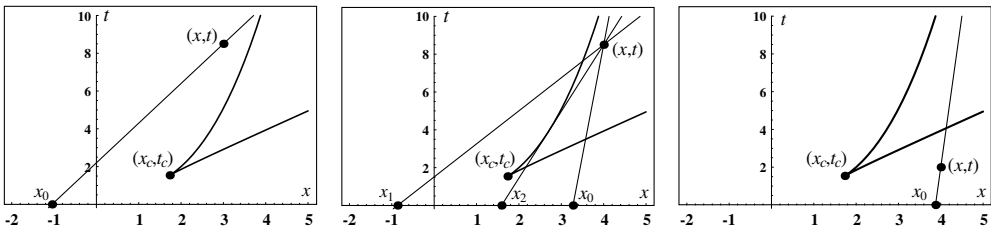

Figure 2. The real rays through real points (x, t) 'inside' and 'outside' the caustic, together with their points of intersection x_j with the $t = 0$ axis. The caustics coalesce at (x_c, t_c). The maintenance of the label x_0 for the single real ray through a point 'outside' the caustic follows from the existence of a branch cut at (x_c, t_c), which is not shown.

Each of these rays gives a separate distinct value for a_0. Hence inside the caustic we have a multivalued solution.

The multivaluedness of the solution of (5) is usually eliminated by introducing a 'shock' into the solution, that is, a region in which the solution u is rapidly varying in x and the expansion (4) is no longer valid. The characteristic solution (7), (8) is valid on either side of the shock, but characteristics are not allowed to pass through the shock, so that there is now only one real ray through each point (see right-hand image in figure 1), and single-valuedness is restored.

For the viscous Burgers' equation (1) the second-derivative ϵu_{xx} term smoothes the discontinuity of the shock. The local behaviour of the solution in the vicinity of the shock is then usually established using the theory of matched asymptotic expansions as follows.

To determine the location of the shock, $x = x_s(t; \epsilon)$ say, we introduce the scaled variable

$$x = x_s + \epsilon X. \tag{12}$$

Writing $u(x, t) = U(X, t)$ the equation becomes

$$-\dot{x_s} U_X + \epsilon U_t + U U_X = U_{XX}, \tag{13}$$

where $\dot{x_s} \equiv \mathrm{d}x_s/\mathrm{d}t$. Now seeking a formal solution of the form

$$U(X, t) \sim \sum_{r=0}^{\infty} A_r(X, t)\epsilon^r, \tag{14}$$

we find $A_0(X, t)$ satisfies

$$-\dot{x_s}\frac{\partial A_0}{\partial X} + A_0\frac{\partial A_0}{\partial X} = \frac{\partial^2 A_0}{\partial X^2}. \tag{15}$$

The boundary conditions on (15) come from matching with the outer solution a_0, and are

$$\lim_{X\to\infty} A_0 = \lim_{x\to x_s^+} a_0, \qquad \lim_{X\to-\infty} A_0 = \lim_{x\to x_s^-} a_0, \tag{16}$$

where the + and − subscripts refer to positions ahead of, or behind, the smoothed shock position, respectively. We shall also assume henceforth that $a_0(x_s^+, t) < a_0(x_s^-, t)$ for finite t.

Integrating (15) once and imposing the boundary conditions as $|X| \to \infty$ gives

$$-\dot{x}_s A_0 + \frac{A_0^2}{2} = \frac{\partial A_0}{\partial X} + C, \tag{17}$$

where C is a constant. Applying the boundary conditions we observe that

$$C = -\dot{x}_s a_0(x_s^+, t) + \frac{a_0(x_s^+, t)^2}{2} \tag{18}$$

$$= -\dot{x}_s a_0(x_s^-, t) + \frac{a_0(x_s^-, t)^2}{2}. \tag{19}$$

Thus we find

$$\dot{x}_s = \frac{a_0(x_s^+, t)^2 - a_0(x_s^-, t)^2}{2(a_0(x_s^+, t) - a_0(x_s^-, t))} = \frac{a_0(x_s^+, t) + a_0(x_s^-, t))}{2}, \tag{20}$$

which is exactly the Rankine–Hugoniot condition associated with mass conservation in the inviscid version of (1). Since a_0 is already known on both sides of the shock (since there is one real characteristic through each point see right hand of figure 1), equation (20) is enough to determine the evolution of the shock. Moreover, (17) can be solved to give the usual (Taylor) shock profile as

$$A_0 = \frac{1}{2}\left\{(a_0(x_s^+, t) + a_0(x_s^-, t)) + (a_0(x_s^+, t) - a_0(x_s^-, t))\tanh\left[\frac{(a_0(x_s^-, t) - a_0(x_s^+, t))}{4}X\right]\right\}. \tag{21}$$

The existence of an infinite array of complex plane singularities (poles) that is associated with the tanh is instructive for what follows.

The final piece of information that should be recorded is that the shock first forms at the cusp $(x_c, t_c) = (\sqrt{3}, 8/\sqrt{27})$ of the two caustics in figure 1, the point at which the outer asymptotic solution first breaks down. This gives the initial condition on (20) as

$$x_s\left(8/\sqrt{27}\right) = \sqrt{3}.$$

As we have indicated in the introduction, for problems such as (1) the behaviour of neither $a_0(x_s^-)$ nor $a_0(x_s^+)$ is singular as the location of the shock is approached. Analytic continuation of $a_0(x_s^+)$ (respectively $a_0(x_s^-)$) to regions with $x < x_s$ ($x > x_s$) does not reveal the existence of the shock: only by the comparison of solutions from $x < x_s$ and $x > x_s$ is the multivaluedness revealed. The shock is taken to exist to get us out of the difficulty of multivaluedness, and the matched asymptotic solution is then shown to be self-consistent.

3. Complex caustics

We now show how the shock arises naturally from an exponential approach. To perform our analysis we shall need to continue the solution analytically to complex values of x. In principle we could also complexify t, but this is not necessary and for simplicity and ease of exposition we restrict ourselves to real $t > 0$.

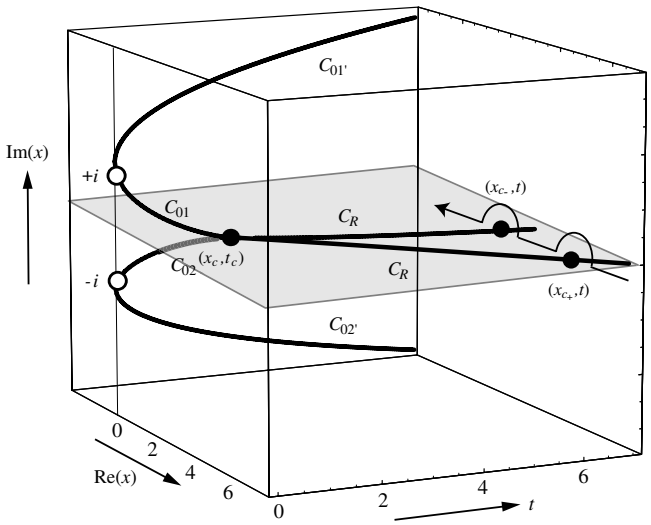

Figure 3. View of the caustics that branch out from the two singularities in the initial data. The caustics $\mathcal{C}_R$ lie in the real x plane (shaded) for $t > t_c$. On these caustics two exponents f_1 and f_2 are equal. On the caustics $\mathcal{C}_{0j}$, $j = 1, 2$, $t < r_c$, the exponents $f_j = 0$. These caustics meet at the (x_c, t_c). Two other caustics $\mathcal{C}_{01'}$ and $\mathcal{C}_{02'}$ recede, without meeting, into the complex x-plane as t increases. Other solutions of the f equation (29), corresponding to exponents $f_{1'} = f_1 - \pi/2$ and (respectively) $f_{2'} = f_2 - \pi/2$, vanish on these caustics. A path of continuation around the real caustics for $t > t_c$ is shown by a thin line.

The real caustics in figure 1 play a crucial role in the exponential-asymptotic approach. However, figure 1 gives only a partial picture: in the three-dimensional space with complex x, $t > 0$ equation (10) generates additional caustics; see figure 3. The identification and location of caustics require the simultaneous satisfaction of two conditions: the coalescence of both the real and the imaginary parts of an exponent. They are objects of codimension 2. In the space of complex x and real t they are therefore one-dimensional curves. The caustics are actually sections of two-dimensional surfaces in the four-dimensional space $(x, t) \in \mathbb{C} \times \mathbb{C}$. In any two-dimensional section with $t =$ constant ($\in \mathbb{R}^+$) and $x \in \mathbb{C}$ the caustics become the conventional turning points of WKB analysis.

At $t = 0$ the complex caustics correspond to two isolated turning points in the complex-x plane, located at $x = \pm i$. These are the singular points in the initial data (3). As t increases the complex caustics approach each other, before coalescing at $(x_c, t_c) = (\sqrt{3}, 8/\sqrt{27})$ and becoming real for $t > 8/\sqrt{27}$. Thus, in this three-dimensional space the caustics chart the time evolution of the singularities that were originally present in the initial data and so will play a significant role in the calculation of the exponential-asymptotic expansions. (For other initial data without singularities at finite locations, for example $u(x, 0) = 4x^3 - x$, the complex, pre-shock, caustics typically diverge to complex ∞ as $t \to 0$.)

It is clear that the codimensionality of a caustic implies that it does not divide three-dimensional ($(x, t) \in \mathbb{C} \times \mathbb{R}$) space into regions 'inside' and 'outside': it is possible to find paths of analytic continuation between and around the caustics in a similar way to one-dimensional WKB theory. One such path circumventing the caustics at (x_{c_+}, t) and (x_{c_-}, t) is indicated in figure 3. When viewed in the complex space $(x, t) \in \mathbb{C} \times \mathbb{R}$ there are actually three rays through every point; it just happens that for real values of x between the two real caustics all three rays originate at real points. For real values of x 'outside' the two real caustics, x_1 and x_2

are complex, and the rays originating from them lie in the complex (x, t)-space, intersecting real space only at the point (x, t) under consideration. Consequently, viewed from a complex-x perspective, there is an apparent multivaluedness in the problem for all (x, t) and we must establish which rays contribute at each point.

For large $x \in \mathbb{R}$, with t bounded, only the ray originating at x_0 does not lead to unbounded growth in the solution. In this limit the initial points of the complex rays on $t = 0$, i.e. x_1 and x_2, approach the singularities $\pm i$ in the initial data (3); we adopt the convention $x_1 \to +i$ and $x_2 \to -i$ (say). The corresponding $a_0(x_j) = 1/(1 + x_j^2)$, $j = 1, 2$, diverge for $x \to \pm\infty$, which is inconsistent with the boundary data. Hence we can say that the only ray which contributes for large x is indeed that originating at x_0, which is consistent with figure 2. With this choice of x_j, x_1 and x_2 coalesce on the real caustics, labelled $\mathcal{C}_R$. However, on the branch of the complex caustic with $\Im x > 0$, x_0 coalesces with x_1. Therefore we label this branch of the caustic $\mathcal{C}_{01}$. On the branch of the complex caustic with $\Im x < 0$, x_0 coalesces with x_2, this branch being labelled $\mathcal{C}_{02}$, see figure 3. The intersection of $\mathcal{C}_{01}$, $\mathcal{C}_{02}$ and $\mathcal{C}_R$ is the critical point $(x_c, t_c) = (\sqrt{3}, 8/\sqrt{27})$. All three corresponding x_j coalesce at the value $x_j = 1/\sqrt{3}$, $j = 0, 1, 2$, and the three rays through this point are coincident.

Having established the nature of all the caustics and the possibility of analytic continuation around them, we may now consider the form of the exponential-asymptotic approximation in each region.

4. Derivation of the exponential-asymptotic template

In this section we demonstrate that the effect of the multivaluedness of $a_0(x, t)$ may be automatically accounted for by using an exponential asymptotics. This is achieved by consideration of exponentially small terms that grow inside $\mathcal{C}_R$ to accurately model the smoothed shock.

To this end, first we seek solutions of Burgers' equation (1) of the form

$$u(x, t; \epsilon) \sim \sum_{r=0}^{\infty} a_r(x, t)\epsilon^r + C\mathrm{e}^{-f(x,t)/\epsilon} \sum_{r=0}^{\infty} a_r^{(1)}(x, t)\epsilon^r, \tag{22}$$

where C does not depend on x or t. Initially we consider $\Re f > 0$, so that the second series is an exponentially small correction. Since (1) is nonlinear, it is clear that terms of $\mathcal{O}\left(\mathrm{e}^{-f/\epsilon}\right)$ generate terms of $\mathcal{O}\left(\mathrm{e}^{-2f/\epsilon}\right)$, which in turn generate terms of order $\mathcal{O}\left(\mathrm{e}^{-3f/\epsilon}\right)$ and $\mathcal{O}\left(\mathrm{e}^{-4f/\epsilon}\right)$ and so on. Thus, in order to achieve balances at these orders, the template for the solution must be extended to the form

$$u(x, t; \epsilon) \sim \sum_{n=0}^{\infty} C^n u^{(n)}(x, t; \epsilon), \tag{23}$$

where

$$u^{(0)}(x, t; \epsilon) \sim \sum_{r=0}^{\infty} a_r(x, t)\epsilon^r, \tag{24}$$

$$u^{(n)}(x, t; \epsilon) \sim \mathrm{e}^{-nf(x,t)/\epsilon} \sum_{r=0}^{\infty} a_r^{(n)}(x, t)\epsilon^r, \qquad n = 1, 2, 3, \cdots. \tag{25}$$

In the language of the theory of resurgence [7, 15, 16] (and references therein) the multiple-series ansatz (23)–(24) of WKBJ-form is called a 'transseries'.

Substitution of (23) into Burgers' equation (1), followed by a balancing at $\mathcal{O}\left(\mathrm{e}^{-nf/\epsilon}\right)$ (up to powers of ϵ), generates equations for the $u^{(n)}$:

$$\frac{\partial u^{(0)}}{\partial t} + u^{(0)}\frac{\partial u^{(0)}}{\partial x} - \epsilon\frac{\partial^2 u^{(0)}}{\partial x^2} = 0, \tag{26}$$

(identical to the original PDE, but where we account only for the non-exponential solutions, namely $u^{(0)}$)

$$\frac{\partial u^{(1)}}{\partial t} + u^{(0)}\frac{\partial u^{(1)}}{\partial x} + u^{(1)}\frac{\partial u^{(0)}}{\partial x} - \epsilon\frac{\partial^2 u^{(1)}}{\partial x^2} = 0, \tag{27}$$

and, for $n = 2, 3, 4, \ldots$,

$$\frac{\partial u^{(n)}}{\partial t} + u^{(0)}\frac{\partial u^{(n)}}{\partial x} + u^{(n)}\frac{\partial u^{(0)}}{\partial x} - \epsilon\frac{\partial^2 u^{(n)}}{\partial x^2} = -\sum_{m=1}^{n-1} u^{(n-m)}\frac{\partial u^{(m)}}{\partial x}. \tag{28}$$

The function $f(x,t)$ satisfies the first-order nonlinear equation

$$\frac{\partial f}{\partial t} + a_0\frac{\partial f}{\partial x} + \left(\frac{\partial f}{\partial x}\right)^2 = 0. \tag{29}$$

The leading orders $a_0^{(n)}$ of each component series $u^{(n)}$ satisfy (5), together with

$$\frac{\partial a_0^{(1)}}{\partial t} + (a_0 + 2f_x)\frac{\partial a_0^{(1)}}{\partial x} + \left(\frac{\partial a_0}{\partial x} - a_1\frac{\partial f}{\partial x} + \frac{\partial^2 f}{\partial x^2}\right)a_0^{(1)} = 0, \tag{30}$$

and, for $n = 2, 3, 4, \ldots$,

$$-n\left(\frac{\partial f}{\partial t} + a_0\frac{\partial f}{\partial x} + n\left(\frac{\partial f}{\partial x}\right)^2\right)a_0^{(n)} = f_x\sum_{m=1}^{n-1}(n-m)a_0^{(m)}a_0^{(n-m)}. \tag{31}$$

Note that the a_0 appearing in (29) is identical to the quantity a_0 in the leading-order behaviour of u_0 in (24): it is therefore $a_0(x_0(x,t))$, which is completely determined by (5), where $x_0(x,t)$ is the real solution of (8) (see the final paragraphs of section 1). The initial conditions and the number of solutions of (29) are defined by reference to the caustics of the inviscid equation, as we explain below.

On the complex caustics, $\mathcal{C}_{01}$ and $\mathcal{C}_{02}$, the function $a_0(x_0)$ has a cube root singularity. (This may be deduced by eliminating x_0 between (8) and (10) to obtain an expression for a_0 involving only x and t.) However, the solution of Burgers' equation with initial boundary data (3) is analytic near the caustics $\mathcal{C}_{01}$ and $\mathcal{C}_{02}$ for $t > 0$.

This apparent paradox can be resolved by consideration of the exponential correction terms on the right-hand side of (22), which can be used to cancel the apparent leading-order singularity. For that to happen we require that (at the very least) the exponents $f(x,t)$ must vanish on the complex caustics, so that the exponential correction terms are of the same order there as the first series in (22). Since there are two such caustics we therefore deduce that there are two possible solutions f_j of (29) satisfying

$$f_j(x,t) = 0 \qquad \text{on} \quad \mathcal{C}_{0j}, \quad j = 1, 2. \tag{32}$$

Hence we deduce that the template for the expansion must be expanded from (23) to include a second set of exponentially prefactored series:

$$u(x,t;\epsilon) \sim u^{(0)}(x,t;\epsilon) + \sum_{n=1}^{\infty} C_1^n u^{(n,1)}(x,t;\epsilon) + \sum_{n=1}^{\infty} C_2^n u^{(n,2)}(x,t;\epsilon), \tag{33}$$

where

$$u^{(0)}(x,t;\epsilon) \sim \sum_{r=0}^{\infty} a_r(x,t)\epsilon^r, \tag{34}$$

$$u^{(n,j)}(x,t;\epsilon) \sim \mathrm{e}^{-nf_j(x,t)/\epsilon} \sum_{r=0}^{\infty} a_r^{(n,j)}(x,t)\epsilon^r, \qquad j=1,2, \quad n=1,2,3,\ldots. \tag{35}$$

Which terms of this new template are present in the expansion of the solution will depend on the values of (x,t). To determine this we need to perform an analytic continuation from a position where the expansions may be tied up using the boundary data as $x \to \infty$.

Note that in the template (33) we have neglected cross terms with exponential orders involving both f_1 and f_2 simultaneously. Strictly speaking these should be present in the full template, but they play little role in the main result and so, for simplicity we have left them out.

The technical details of these calculations may be found in the following section (section 5). The exponential approach is general and does not rely on any *a priori* knowledge of the behaviour of the solution or, including the existence, or otherwise, of a shock, or on information from matched asymptotics. At a first pass, a reader may skip this section and jump to the discussion of the implications of the approach in section 6.

We next summarize the results of our exponential-asymptotic investigation. Which contributions are present in each region of the complex x-plane is summarized later in figure 5.

The key coefficients that we require are evaluated in section 5. It is convenient to express these coefficients in terms of the ray coordinates (x_0, x_j). We find that the f_j, $j=1,2$, are given by

$$f_j\left(x(x_0,x_j),t(x_0,x_j)\right) = \frac{1}{2}\int_{x_0}^{x_j} a_0(z)\,\mathrm{d}z - \frac{1}{4}\left(a_0(x_0)+a_0(x_j)\right)(x_j-x_0), \tag{36}$$

where $x(x_0,x_j), t(x_0,x_j)$ are defined by the inversion of ray equations

$$x = x_0 + a_0(x_0)t, \qquad x = x_j + a_0(x_j)t. \tag{37}$$

Note that on the other pair of complex caustics $\mathcal{C}_{01'}$ and $\mathcal{C}_{02'}$ two other solutions of (29), f_1' and f_2', respectively vanish. These are related to f_1 and f_2, by the following result:

$$f_j' \equiv f_j(x_0,x_j') = f_j(x_0,x_j) + \frac{(-1)^j}{2}\oint_{\{(-1)^{j-1}i\}} a_0(z)\,\mathrm{d}z = f_j(x_0,x_j) - \pi/2.$$

Here x_j' is the image of x_j on the next Riemann sheet of the x_j plane as x moves from $\mathcal{C}_{0j}$ to $\mathcal{C}_{0j'}$[6].

The term in the first subdominant expansion involving f_1 is also required and this can be expressed in ray coordinates as

$$a_0^{(1,1)}(x_0,x_1) = (a_0(x_1)-a_0(x_0))\sqrt{\frac{a_0(x_1)-a_0(x_0)-a_0'(x_0)(x_1-x_0)}{a_0(x_1)-a_0(x_0)-a_0'(x_1)(x_1-x_0)}}. \tag{38}$$

When x is real and $x > x_{c^+}$, we find from the boundary data as $x \to \infty$ that $C_1 = C_2 = 0$, so that

$$u(x,t;\epsilon) \sim u^{(0)}(x,t;\epsilon) = a_0(x,t) + O(\epsilon) \tag{39}$$

represents the complete asymptotic expansion. This representation remains valid in a region of $(x,t) \in \mathbb{C}\times\mathbb{R}$ bounded by Stokes surfaces emerging from x_{c^+}, above and below the

[6] The relationship between exponents is analogous to that found in a WKB treatment of the quantum barrier problem where the $\mathcal{C}_{0j}$ and $\mathcal{C}_{0j'}$ are the classical turning points of the motion. The factor $\pi/2$ above is the value of the phase integral around a classically forbidden periodic orbit between the turning points.

real x-plane. After the caustic is crossed, for a region just to the left of the caustic, $x_{c^+} - \delta < x < x_{c^+}$, $0 < \delta \ll 1$ with $t > t_c$, we have

$$0 < f_1 < f_2. \tag{40}$$

Furthermore an infinite number of exponentially small contributions is then present and an expression of the form (33) holds with $C_1 = K_{01} \neq 0$, that is

$$u(x,t;\epsilon) \sim u^{(0)}(x,t;\epsilon) + \sum_{n=1}^{\infty} K_{01}^n u^{(n,1)}(x,t;\epsilon), \tag{41}$$

The Stokes constant K_{01} is shown below to be unity.

When $x \in \mathbb{R}$, $x \in (x_{c_-}, x_{c_+})$, moving further away from x_{c_+}, $f_1(x,t)$ may become zero. There is thus the possibility that the leading-order terms arising from all series prefactored by exponentials involving $f_1(x,t)$ may grow to $\mathcal{O}(1)$ and interact with $a_0(x,t)$. Extracting the leading orders of each transseries [7, 15] we have

$$u(x,t;\epsilon) \sim a_0(x,t) + \sum_{n=1}^{\infty} K_{01}^n \mathrm{e}^{-nf_1(x,t)/\epsilon} a_0^{(n,1)}(x,t). \tag{42}$$

Crucially, there is an important relationship between the $a_0^{(n,1)}(x,t)$ in (42). To see this we combine (31) and (29) to obtain for $n = 2, 3, 4, \ldots$

$$-n(n-1)\frac{\partial f_1}{\partial x} a_0^{(n,1)} = \sum_{m=1}^{n-1} (n-m) a_0^{(m,1)} a_0^{(n-m,1)}, \tag{43}$$

from which it follows that

$$a_0^{(n,1)} = \left(a_0^{(1,1)}\right)^n \left(-2\frac{\partial f_1}{\partial x}\right)^{1-n}. \tag{44}$$

This relationship allows us to sum the series in (42) to arrive at

$$u(x,t;\epsilon) \sim a_0(x,t) + \frac{2K_{01} a_0^{(1,1)}(x,t)(\partial f_1/\partial x)\mathrm{e}^{-f_1/\epsilon}}{2(\partial f_1/\partial x) + K_{01} a_0^{(1,1)}(x,t)\mathrm{e}^{-f_1/\epsilon}}, \tag{45}$$

as $\epsilon \to 0+$.

We show below that $K_{01} = 1$.

That an explicit summation is possible here is a special feature of the class of problems under consideration. In more general nonlinear PDE systems, when explicit knowledge of the relevant coefficients prevents an explicit summation, the transseries can often still be resummed by applying a Z-transform to the corresponding recurrence relations (31) governing the $a_0^{(n)}$. This approach avoids the need to know the $a_0^{(n)}$ explicitly and is explained in [9].

The result (45) is valid everywhere in the region where $\Re f_1 > 0$ and may be analytically continued to the region where $\Re f_1 \leqslant 0$. The apparent inconsistency of the inclusion of exponentially small terms before terms involving algebraic powers ($a_1(x,t)\epsilon$, etc) is explained by this fact. In fact, the position of the smoothed shock wave is given by the contour $f_1 = 0$, which coincides with the location given by the Rankine–Hugoniot condition (20), but avoids the requirement of having to impose or solve the latter.

The expression (45) forms the basis for the leading-order exponential-asymptotic approximation to the solution of the Burgers' problem (1)–(3) throughout the region $x_{c_-} < x < x_{c_+}$, $t > t_c$.

From the definition of f_1, (36), we have

$$\frac{\partial f_1}{\partial x} = \frac{1}{2}\left(a_0(x_1) - a_0(x_0)\right), \tag{46}$$

so that inside the caustic, either side of the smoothed shock, to leading order in ϵ (45) becomes

$$u(x,t;\epsilon) \sim a_0(x_0) + \mathcal{O}(\epsilon), \qquad f_1 > 0, \tag{47}$$

$$\sim a_0(x_1) + \mathcal{O}(\epsilon), \qquad f_1 < 0, \tag{48}$$

when expressed in ray coordinates. Note that $a_0(x_1)$ automatically becomes $a_0(x_0)$ by the branch-cut-related relabelling of x_1 to x_0 on traversing the caustic to regions where $x < x_{c_-}$ (compare the definitions of the x_j 'inside' and 'outside' the caustic in figure 2). Hence for $t > t_c$ equation (45) resolves the multivaluedness and hence the ambiguity in representation. It can be used as a leading-order uniform approximation to the solution of Burgers' equation throughout the real region 'inside' the caustic. Moreover, the shock is automatically incorporated in the representation.

In fact it is not too difficult to see that the matched asymptotics result (21) can be obtained from the exponential-asymptotic result (45) by replacing f_1/ϵ by its leading-order approximation $X\partial f_1/\partial x = \epsilon^{-1}(x - x_s(t))\partial f_1/\partial x$, using (46) and identifying $a_0(x_0)$ with $a_0(x_s^+, t), a_0(x_1)$ with $a_0(x_s^-, t)$. This suggests that the exponential-asymptotic result is actually valid in a wider region of validity than the matched asymptotics.

Clearly, had we pursued a Cole–Hopf approach to the problem, we would have arrived at (45) by a shorter route. However, unlike Cole–Hopf, the current approach has not fundamentally relied on the fact that we are solving Burgers' equation and is accordingly more general [11].

Note that we have still to resolve the fundamental question of this paper: why is the shock not a caustic? The wider region of validity of the exponential-asymptotic result will be crucial to the resolution.

5. Derivation of the exponential-asymptotic coefficients

5.1. Determination of the exponents f_j

In this section we derive the most important coefficients contained in the above templates for the exponential-asymptotic expansions, these being the $f_j(x,t)$ and $a_0^{(1,j)}$. These quantities could be determined easily from the Cole–Hopf representation of the solution, but here we illustrate their derivation using techniques applicable to more general nonlinear PDEs.

In order to determine the solutions f_j of (29) subject to conditions (32) on the appropriate caustic, a natural change of coordinates is suggested by the rays of the inviscid equation (5) that generate the caustics. Three rays originating from x_0, x_1 and x_2 at $t = 0$ pass through each (x,t). To determine f_j, we map (x,t) to new variables (x_0, x_j). Without loss of generality we carry out the analysis for $j = 1$ and write $x = x(x_0, x_1)$ and $t = t(x_0, x_1)$ using the equations of the relevant rays

$$x = x_0 + a_0(x_0)t, \qquad x = x_1 + a_0(x_1)t \tag{49}$$

as the map. This mapping is invertible to give x_0 and x_1 for all (x,t) except those on $\mathcal{C}_{01}$. However we only need to find f_1 away from the caustic, since we already know that $f_1 = 0$ on that caustic. Hence the map (49) is well-defined in the regions of interest.

For the sake of brevity in what follows, we now introduce the function

$$h(x_0, x_1) = \frac{\partial x_0}{\partial x} = \frac{a_0(x_1) - a_0(x_0)}{a_0(x_1) - a_0(x_0) - a_0'(x_0)(x_1 - x_0)}. \tag{50}$$

Note that with this definition

$$h(x_1, x_0) = \frac{\partial x_1}{\partial x}. \tag{51}$$

Hence, the x and t partial derivatives map from (x, t) to (x_0, x_1) according to

$$\frac{\partial}{\partial x} = h(x_0, x_1)\frac{\partial}{\partial x_0} + h(x_1, x_0)\frac{\partial}{\partial x_1},$$
$$\frac{\partial}{\partial t} = -a_0(x_0)h(x_0, x_1)\frac{\partial}{\partial x_0} - a_0(x_1)h(x_1, x_0)\frac{\partial}{\partial x_1}.$$

Thus, using (49)–(52), the equation (29) determining f_1 becomes

$$(a_0(x_0) - a_0(x_1))\, h(x_1, x_0)\frac{\partial f_1}{\partial x_1} + \left(h(x_0, x_1)\frac{\partial f}{\partial x_0} + h(x_1, x_0)\frac{\partial f}{\partial x_1}\right)^2 = 0, \tag{52}$$

which can be rewritten in the symmetric form

$$\frac{\partial f_1/\partial x_1}{\partial b/\partial x_1} + \left(\frac{\partial f_1/\partial x_0}{\partial b/\partial x_0} + \frac{\partial f_1/\partial x_1}{\partial b/\partial x_1}\right)^2 = 0, \tag{53}$$

where

$$b(x_0, x_1) = (a_0(x_0) + a_0(x_1))\,(x_1 - x_0) + 2\int_{x_1}^{x_0} a_0(z)\,\mathrm{d}z, \tag{54}$$

so that

$$\frac{\partial b}{\partial x_0} = a_0'(x_0)(x_1 - x_0) + a_0(x_0) - a_0(x_1), \tag{55}$$
$$\frac{\partial b}{\partial x_1} = a_0'(x_1)(x_1 - x_0) + a_0(x_0) - a_0(x_1). \tag{56}$$

On the caustic $\mathcal{C}_{01}$, where $x_1 = x_0$, we have the boundary condition

$$f_1(x_0, x_0) = 0. \tag{57}$$

We note from (54) that $b(y, y) = 0$. Hence, on $\mathcal{C}_{01}$, we observe that b, like f_1, vanishes. Thus the solution of (53) satisfying (57) must be a multiple of b:

$$f_1(x_0, x_1) = \alpha b(x_0, x_1). \tag{58}$$

Substituting (58) in (53), we find (rejecting the trivial solution $\alpha = 0$) that $\alpha = -\frac{1}{4}$. Hence by comparison of (58) and (54) we finally obtain

$$f_1\,(x(x_0, x_1), t(x_0, x_1)) = \frac{1}{2}\int_{x_0}^{x_1} a_0(z)\,\mathrm{d}z - \frac{1}{4}\,(a_0(x_0) + a_0(x_1))\,(x_1 - x_0). \tag{59}$$

A similar analysis, based on $\mathcal{C}_{02}$, holds for f_2 , so that we can write

$$f_j\left(x(x_0, x_j), t(x_0, x_j)\right) = \frac{1}{2}\int_{x_0}^{x_j} a_0(z)\,\mathrm{d}z - \frac{1}{4}\left(a_0(x_0) + a_0(x_j)\right)(x_j - x_0), \tag{60}$$

$j = 1, 2$. Recall that on the real caustics $\mathcal{C}_R$, x_1 and x_2 coalesce. From (60) we may thus deduce that

$$f_1(x, t) = f_2(x, t) \qquad \text{on } \mathcal{C}_R. \tag{61}$$

It is clear from the form of the template solution (33) that we could interpret the leading-order expansion $u^{(0)}$ as having an exponential prefactor $\mathrm{e}^{-f(x,t)/\epsilon}$ with $f(x, t) = 0$ for all (x, t). This is actually the trivial solution with $\alpha = 0$ above. In what follows, by analogy with the definitions of f_1 and f_2 in (60), it will be convenient to label this solution as f_0.

5.2. *Determination of* $a_0^{(1,1)}$

Our next goal is to determine the leading coefficient $a_0^{(1,1)}$ in the expansion prefactored by the exponential $\mathrm{e}^{-f_1/\epsilon}$. It satisfies the first-order linear homogeneous PDE (30) with f replaced by f_1, that is the amplitude equation

$$\frac{\partial a_0^{(1,1)}}{\partial t} + \left(a_0(x_0) + 2\frac{\partial f_1}{\partial x}\right)\frac{\partial a_0^{(1,1)}}{\partial x} + \left(\frac{\partial a_0(x_0)}{\partial x} - a_1\frac{\partial f_1}{\partial x} + \frac{\partial^2 f_1}{\partial x^2}\right)a_0^{(1,1)} = 0. \tag{62}$$

To solve (62) we see that first we require a_1, which from (6) satisfies

$$\frac{\partial a_1}{\partial t} + a_0(x_0)\frac{\partial a_1}{\partial x} + \frac{\partial a_0(x_0)}{\partial x}a_1 = \frac{\partial^2 a_0(x_0)}{\partial x^2}, \qquad \text{with} \quad a_1(x,0) = 0. \tag{63}$$

Converting to (x_0, x_1) coordinates, we have from (52) that

$$\frac{\partial a_0(x_0)}{\partial x} = h(x_0,x_1)a_0'(x_0), \qquad \frac{\partial^2 a_0(x_0)}{\partial x^2} = h^3(x_0,x_1)a_0''(x_0). \tag{64}$$

Thus the homogeneous part of (63) becomes

$$\frac{\partial \tilde{h}}{\partial t} + a_0(x_0)\frac{\partial \tilde{h}}{\partial x} + \frac{\partial a_0(x_0)}{\partial x}\tilde{h} = \left(a_0(x_0) - a_0(x_1)\right)h(x_1,x_0)\frac{\partial \tilde{h}}{\partial x_1} + a_0'(x_0)h(x_0,x_1)\tilde{h} = 0, \tag{65}$$

and we find that the complementary function is $\tilde{h}(x_0,x_1) = \phi(x_0)h(x_0,x_1)$, where $\phi(x_0)$ is arbitrary. To complete the general solution we use variation of parameters and obtain $-a_0''(x_0)h^2(x_0,x_1)/a_0'(x_0)$ as a particular integral for (63). The initial condition requires $a_1(x,0) = 0$. We recall from above that as $t \to 0^+$ then $x_0 \to x$, $x_1 \to i$, hence $a_0(x_1) \to \infty$ and $h(x_0,x_1) \to 1$. Thus

$$a_1(x_0,x_1) = \frac{a_0''(x_0)}{a_0'(x_0)}\left(h(x_0,x_1) - h^2(x_0,x_1)\right) \tag{66}$$

is the solution of (63) satisfying the required initial condition.

We now use (66) and the observation that

$$\begin{aligned}\frac{\partial f_1}{\partial x} &= \frac{1}{2}\left(a_0(x_1) - a_0(x_0)\right),\\ \frac{\partial^2 f_1}{\partial x^2} &= \frac{1}{2}\left(a_0'(x_1)h(x_1,x_0) - a_0'(x_0)h(x_0,x_1)\right)\end{aligned} \tag{67}$$

in (62) and obtain the general solution

$$a_0^{(1,1)}(x_0,x_1) = \tilde{\phi}(x_1)\left(a_0(x_1) - a_0(x_0)\right) \times \sqrt{\frac{a_0(x_1) - a_0(x_0) - a_0'(x_0)(x_1 - x_0)}{a_0(x_1) - a_0(x_0) - a_0'(x_1)(x_1 - x_0)}}, \tag{68}$$

where $\tilde{\phi}(x_1)$ is arbitrary.

It is important to note that the initial condition $u(x,0) = a_0(x_0)$ does not result directly in any initial condition for $a_0^{(1,1)}$ and hence an equation for $\tilde{\phi}(x_1)$. This is because as $t \to 0^+$, $f_1 \to +\infty$. Hence the exponentially subdominant contribution $\exp(-f_1/\epsilon)\left(a_0^{(1,1)} + \mathcal{O}(\epsilon)\right)$ vanishes at $t = 0$ and so the initial condition is satisfied for any finite value of $a_0^{(1,1)}(x,0)$. Consequently, at first sight, we appear to have an indeterminacy in the problem. In fact this is not the case, since we can use techniques of exponential asymptotics to derive $\tilde{\phi}(x_1)$ in the following way.

It transpires that $\tilde{\phi}(x_1)$ in (68) is constant. Our method to show this is based on the factorial-over-power, exponential-asymptotic, ansatz [8] that if $|f_1| < |f_2|$ then as $r \to \infty$

$$a_r(x_0, x_1) \sim \frac{a_0^{(1,1)}(x_0, x_1)}{2\pi i} \frac{\Gamma(r+\beta)}{(f_1(x_0, x_1))^{r+\beta}}. \tag{69}$$

This ansatz can easily be justified *a posteriori* by the Borel transform approach outlined in the next section and in the appendix. We will study the growth of the coefficients $a_r(x_0, x_1)$ near the caustic $\mathcal{C}_{01}$, that is, when $x_1 \to x_0$ and $|f_1| \to 0$. We observe from (59) that

$$f_1(x_0, x_1) \sim -\tfrac{1}{24} a_0''(x_0)(x_1 - x_0)^3, \qquad \text{as} \quad x_1 \to x_0, \tag{70}$$

and from (68) that

$$a_0^{(1,1)}(x_0, x_1) \sim \mathrm{i}\tilde{\phi}(x_0) a_0'(x_0)(x_1 - x_0), \qquad \text{as} \quad x_1 \to x_0. \tag{71}$$

We now know the dominant behaviour of the right-hand side of (69) as $x_1 \to x_0$. To balance this we will also determine the dominant behaviour for the left-hand side of (69). First we note from (66) that

$$a_1(x_0, x_1) \sim -4 \frac{a_0'(x_0)}{a_0''(x_0)} (x_1 - x_0)^{-2}, \qquad \text{as} \quad x_1 \to x_0. \tag{72}$$

We shall also need

$$\frac{\partial}{\partial x}(x_1 - x_0)^{-m} \sim 4m \frac{a_0'(x_0)}{a_0''(x_0)} (x_1 - x_0)^{-m-2}, \tag{73}$$

$$\frac{\partial^2}{\partial x^2}(x_1 - x_0)^{-m} \sim 16m(m+2) \left(\frac{a_0'(x_0)}{a_0''(x_0)} \right)^2 (x_1 - x_0)^{-m-4}, \tag{74}$$

as $x_1 \to x_0$, which follow from (52).

We write $a_r = h(x_0, x_1) c_r(x_0, x_1)$ and obtain from (6) the equation for c_r as

$$(a_0(x_0) - a_0(x_1))\, h(x_1, x_0) h(x_0, x_1) \frac{\partial c_r}{\partial x_1} = \frac{\partial^2 a_{r-1}}{\partial x^2} - \sum_{s=1}^{r-1} a_{r-s} \frac{\partial a_s}{\partial x}. \tag{75}$$

The dominant behaviours (70) and (71) suggest the local form

$$a_r(x_0, x_1) \sim K_r (x_1 - x_0)^{1-3r}, \qquad \text{as} \quad x_1 \to x_0, \qquad r = 1, 2, 3, \ldots. \tag{76}$$

This can be proved by induction as follows. We substitute (76) into the right-hand side of (75) and obtain the leading-order behaviour

$$\frac{\partial c_r}{\partial x_1} \sim \left(K_{r-1} \frac{4(3r-4)(3r-2)}{a_0'(x_0)} - \sum_{s=1}^{r-1} K_{r-s} K_s \frac{a_0''(x_0)(3s-1)}{a_0'(x_0)^2} \right) (x_1 - x_0)^{1-3r}, \tag{77}$$

as $x_1 \to x_0$. We integrate this result with respect to x_1 and multiply by $h(x_0, x_1)$ to obtain (76), with

$$K_r = -K_{r-1} \frac{8(3r-4)}{a_0''(x_0)} + \sum_{s=1}^{r-1} K_{r-s} K_s \frac{2(3s-1)}{a_0'(x_0)(3r-2)}, \qquad r = 2, 3, 4, \ldots. \tag{78}$$

Since (76) holds for $r = 1$ with $K_1 = -4a_0'(x_0)/a_0''(x_0)$ (see (72)) it will then hold for all $r \geqslant 1$.

An examination of the growth with r of the K_r generated by (78) suggests that we should write

$$K_r = k_r a_0'(x_0) \frac{\Gamma(r)}{\left(-\frac{1}{24} a_0''(x_0)\right)^r}, \tag{79}$$

whence we find $k_1 = \frac{1}{6}$, $k_2 = k_3 = \frac{5}{36}$ and

$$k_r = k_{r-1} + \sum_{s=2}^{r-2} 2k_{r-s}k_s \frac{(3s-1)\Gamma(s)\Gamma(r-s)}{(3r-2)\Gamma(r)}, \qquad r = 4, 5, 6, \ldots. \tag{80}$$

The sequence $k_1, k_2, k_3, \cdots$ converges to a limit that can be computed numerically. In general, this limit could, in principle, be any number, real or complex. However, it is possible here to compute the limit as $k_\infty = 1/(2\pi)$.

Comparing (69) with (76) and (79), we deduce that $\beta = 0$ in (69) and hence

$$a_r(x_0, x_1) \sim \frac{a_0'(x_0)}{2\pi} \frac{\Gamma(r)}{\left(-\frac{1}{24}a_0''(x_0)\right)^r} (x_1 - x_0)^{1-3r} \tag{81}$$

$$\sim \frac{a_0^{(1,1)}(x_0, x_1)}{2\pi i} \frac{\Gamma(r)}{(f_1(x_0, x_1))^r}, \tag{82}$$

as $x_1 \to x_0$ and $r \to \infty$. Finally we use the local expressions (70) for f_1 and (71) for $a_0^{(1,1)}$ in (82) and, by comparison (81), we deduce that $\tilde{\phi}(x_1) = 1$.

We conclude that

$$a_0^{(1,1)}(x_0, x_1) = (a_0(x_1) - a_0(x_0)) \sqrt{\frac{a_0(x_1) - a_0(x_0) - a_0'(x_0)(x_1 - x_0)}{a_0(x_1) - a_0(x_0) - a_0'(x_1)(x_1 - x_0)}}. \tag{83}$$

This results holds for all values of x_0 and x_1. Note that in this section we have determined $a_0^{(1,1)}$ in such a way that (82) holds. Consequently, the Stokes multiplier K_{01} in (41) is seen to be unity.

6. Analytic continuation around the caustics: why is a shock not a caustic?

We now turn to the central question of the paper: why is a shock not a caustic? To clarify this we will need to consider an analytic continuation around the actual caustics surrounding the shock region to examine how the asymptotic expansion might change during the process. This is conveniently done by writing the solution of the problem as a Borel transform and appealing to the movement of singularities of the Borel transform of the solution $u^{(0)}(x, t; \epsilon)$, which is defined in terms of the Taylor series

$$y^{(0)}(x, t; \tau) = \sum_{r=0}^{\infty} \frac{a_r(x, t)}{r!} \tau^r. \tag{84}$$

This series converges for $|\tau| < \min(|f_1(x, t)|, |f_2(x, t)|)$. The connection between $u^{(0)}(x, t; \epsilon)$ and $y^{(0)}(x, t; \tau)$ is the Laplace transform

$$u^{(0)}(x, t; \epsilon) = \epsilon^{-1} \int_0^{\infty} \mathrm{e}^{-\tau/\epsilon} y^{(0)}(x, t; \tau)\, \mathrm{d}\tau. \tag{85}$$

This integral representation holds for real (x, t) outside the real caustics.

The complex τ plane is called the 'Borel plane' [7], [14].

When viewed from $\tau = 0$, it may be deduced from the template (33) that branch points exist at

$$\tau = n f_j(x, t), \qquad j = 1, 2, \quad n = 1, 2, 3 \ldots. \tag{86}$$

As (x, t) are varied, these branch points move around the Borel plane and, at a Stokes Phenomenon, can interact with the integration contour of $u^{(0)}$ in (85) or, at a caustic, coalesce. If a Stokes phenomenon takes place, the contour snags on a branch point nf_j, and generates

an additional integral contribution of a similar type to (85). The small ϵ asymptotics of that integral generates the exponential corrections $u^{(n,j)}(x,t;\epsilon)$ in (33).

A necessary condition for a Stokes phenomenon to occur is that a singularity $nf_j(x,t)$ is on the same Riemann sheet as the integration contour in (85) . Similarly, for a caustic to occur, all the coalescing singularities must be on the same sheet.

Thus to obtain a full understanding of the exponential asymptotics, and to appreciate fully the subtleties of the formation of the shock wave, we need to study the Riemann-sheet structure of this Borel plane. A more detailed discussion of the full singularity structure can be found in appendix A. We shall now assume the structure outlined there and consider the analytic continuation of the transseries expansion in the real plane from regions 'outside' the $\mathcal{C}_R$ to 'inside'. Without loss of generality, we shall perform this continuation at a constant $t > 8/\sqrt{27}$. The space of continuation is therefore a complex x-plane in which the caustics degenerate to a pair of turning points. Due to symmetry of the initial conditions as $|x| \to \infty$ we shall also initially just consider the continuation around the turning point with the largest value of $\Re\, x$. We label this point x_{c+}.

We take a path in the complex x-plane along the points x_A, x_B, ...; see figure 4. This path is chosen to be complex to avoid any potentially singular behaviour in the exponentially small transseries $u^{(n,1)}$ and $u^{(n,2)}$, which nevertheless will play a vital role inside the caustic region. It is obviously possible to obtain a uniform asymptotic approximation across the caustic involving special functions. However, we are interested here in the more fundamental exponential-asymptotic behaviour that underpins the matched asymptotic approach.

Surrounding the central diagram of the complex x-plane in figure 4, we provide snapshots of the locations of the singularities as viewed from $\tau = f_0$ in the Borel plane at the positions x_A, x_B, ... As we move around the complex-x plane, the arrays of singularities will pivot about $f_0 = 0$. In figure 4 we also plot sections through the Stokes surfaces $S_{i>j}$ across which asymptotic contributions involving f_i can switch on f_j. These are defined by

$$S_{i>j} = \left\{(x,t) : f_j(x,t) - f_i(x,t) > 0\right\}. \tag{87}$$

In this constant t-section of the parameter space, the codimension-1 Stokes surfaces become curves.

Note that at the turning point x_{c+}, $f_1 = f_2 > 0$. (This turning point does not directly involve f_0.) Thus the Stokes lines $S_{0>1}$ and $S_{0>2}$ both pass through the turning point inertly and f_0 dominates f_1 and f_2, respectively, all along these lines in the vicinity of x_{c+}. Conversely, the Stokes lines $S_{1>2}$ and $S_{2>1}$ sprout at angles of $2\pi/3$ from x_{c+} (reflecting the Airy-type nature of the simple coalescence of singularities in the Borel plane).

The reader might expect from appendix A that we should also have to consider Stokes phenomena between nf_1 and mf_2 where n and m are positive integers. From (A.5) it follows that $y^{(n,1)}(x,t;\tau)$ sees only singularities at $(m+n)f_1$ and $nf_1 + mf_2$. The first group of these singularities can cause a Stokes phenomenon only when f_1 is real and positive, and this is precisely the Stokes line $S_{0>1}$. The second group of these singularities can cause a Stokes phenomenon only when f_2 is real and positive, and this is precisely the Stokes line $S_{0>2}$. Hence, we have to consider the Stokes lines $S_{0>1}$, $S_{0>2}$, $S_{1>2}$ and $S_{2>1}$ only.

From [5, 6, 10] we know that whenever there are three or more possible asymptotic contributions of type (24), consideration of Stokes surfaces alone is not sufficient to determine the asymptotic structure in ϵ of functions dependent on parameters (x,t). It is also necessary to consider the effect of so-called *higher-order Stokes surfaces*, across which the Riemann-sheet structure of the Borel plane can change. A higher-order Stokes surface occurs when f_0, f_1 and f_2 are collinear in the Borel plane. Such a conjunction occurs at values of (x,t) that satisfy

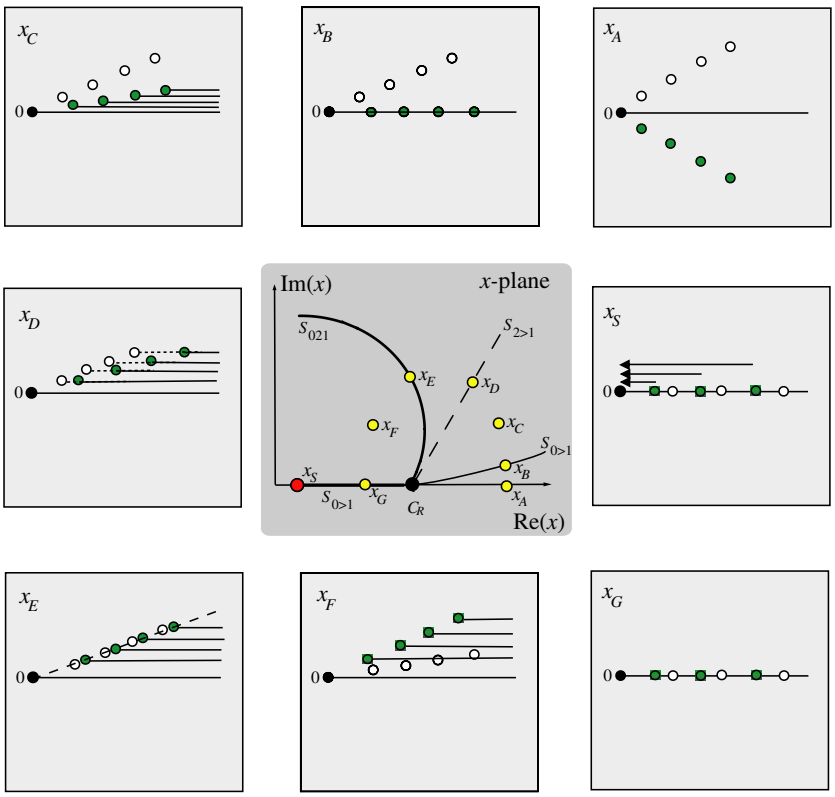

Figure 4. The location of significant points along the path of analytic continuation (in a complex x, constant t section) in the neighbourhood of the caustic x_{c+} (central panel), surrounded by cartoons of the associated Borel planes at each location. Singularities in the Borel plane are denoted by circles. The singularity 0 at the origin of the Borel planes corresponds to the exponent $f_0 = 0$ of the leading-order expansion $u^{(0)}(x, t; \epsilon)$. The array of darker circles denotes the singularities located at $nf_1(x, t), n = 1, 2, 3 \ldots$. The lighter circles denote the singularities located at $nf_2(x, t)$, $n = 1, 2, 3 \cdots$. The integration contours of those which are contributing terms to the transseries at each point are shown as lines extending horizontally to $+\infty$. The Stokes curves between contributions involving f_i and f_j are denoted by $S_{i>j}$ and the higher-order Stokes curve S_{021} is drawn in bold.

the condition

$$S_{0jk} = \left\{ (x, t) : \frac{f_j(x, t) - f_0(x, t)}{f_k(x, t) - f_j(x, t)} \in \mathbb{R} \right\}, \qquad j \neq k. \tag{88}$$

Higher-order Stokes surfaces have the same codimension as Stokes surfaces and so in the complex-x plane they are also curves. A higher-order curve S_{021} exists for (x, t) in the locality of x_{c_+} and this is shown in figure 4.

Note that a branch cut also emanates from $x > x_{c+}$. However, in what follows we can avoid all interaction with it, and so for simplicity we have not included it in figure 4.

We now consider the full asymptotic representation of the solutions of Burgers' equation (1) satisfying (3) on a path of analytic continuation that starts on the real-x axis outside the caustic region where $x > x_{c+}$. We pick a general point x_A, and aim to continue to $x < x_{c+}$ in the complex-x plane.

In order to satisfy the decay conditions on u as $|x| \to \infty$, that is (3), comparison of the full template for the expansion (33) reveals that $C_1 = C_2 = 0$. Hence at x_A we have

$$u(x_A, t; \epsilon) \sim u^{(0)}(x_A, t; \epsilon) \tag{89}$$

as the complete asymptotic expansion.

At x_B we cross the Stokes line $S_{0>1}$. Here the array of singularities nf_1, $n = 1, 2, 3, \ldots$ lines up horizontally with the direction of Borel integration. Consequently a nonlinear Stokes phenomenon takes place involving all the nf_1, see [15] and/or [16]. After crossing the line (at point $x = x_C$) the asymptotics is now a transseries that takes the form

$$u(x, t; \epsilon) \sim u^{(0)}(x, t; \epsilon) + \sum_{n=1}^{\infty} K_{01}^n u^{(n,1)}(x, t; \epsilon), \tag{90}$$

where K_{01} is a Stokes constant. In the final part of section 5.2 we have shown that $K_{01} = 1$.

A Stokes phenomenon could also happen between nf_2 and $nf_2 + mf_1$ at x_B since here $(nf_2 + mf_1) - nf_2 > 0$. However, at x_B contributions from nf_2 are absent in the transseries for u. Consequently the $(nf_2 + mf_1)$ cannot cross any integration contour from nf_2 and so no Stokes phenomenon actually takes place. From the point of view of $u^{(n,2)}$ this is, in the terminology of [10], an active, but irrelevant, Stokes curve.

At x_D we encounter the Stokes line $S_{2>1}$. At this point $f_1 - f_2 > 0$ and so there is potential for a Stokes phenomenon to take place between contributions involving f_1 and f_2. However, as above, the singularity f_2 is not contributing to the transseries expansion of the function we are interested in at x_D. Hence no Stokes phenomenon between f_2 and f_1 actually takes place and this is again an irrelevant Stokes curve.

At x_E, we encounter the higher-order Stokes line S_{021}. On this curve f_0, f_1 and f_2 are collinear. It then follows that all the singularities (A.3), (A.5), (A.6) are collinear. The collinearity is not in the direction of the Borel integration. From [10] we know that this type of collinearity is characteristic of the higher-order Stokes phenomenon, except that here we see that rather than having a finite number of collinear singularities, we must deal here with infinite sets. Since $|f_1| > |f_2|$, on the line of collinearity in the Borel plane the singularity f_2 lies in between f_0 and f_1. As we cross the higher-order Stokes line, when viewed from f_0, the singularity at f_1 moves across a cut from f_2 and onto a different Riemann sheet from f_0. Similarly, on the line of collinearity in the Borel plane the singularity $nf_1 + f_2$ lies in between each pair of singularities nf_1 and $(n+1)f_1$. When we cross the higher-order Stokes line, when viewed from nf_1 the singularity at $(n+1)f_1$ will move across a cut from $nf_1 + f_2$ and onto a different Riemann sheet from nf_1.

Hence we may conclude that here an infinite number of Riemann sheets is associated with the higher-order Stokes phenomenon. There then follows the possibility that after the higher-order Stokes line is crossed, all the singularities in the array $f_1, 2f_1, 3f_1, \ldots$ are not directly visible from the original expansion point f_0, and that nf_1 can no longer see mf_1, $m \neq n$. In what follows, we assume that this is indeed the case and will justify this by reference to the formation of the smoothed shock inside the caustic region.

At x_F, the arrays are no-longer collinear with one another. However, the nf_1 are still collinear with f_0: just because they might be on different Riemann sheets, this does not grant them the autonomy to move independently.

At x_G, where x is real, but $x < x_{c+}$, f_0 and the arrays nf_1, mf_2 are all again collinear, this time along the horizontal direction of Borel integration and with $0 < f_1 < f_2$. A Stokes line therefore potentially exists between f_0 and the nf_1. However, since we have assumed that the nf_1 are now all on different Riemann sheets from f_0, they are invisible to f_0 and cannot cross the actual Borel integration contour, which is anchored at f_0 on the principal Riemann

sheet. Thus the Stokes line $S_{0>1}$ is inactive and no Stokes phenomenon between f_0 and any nf_1 takes place. There is also the possibility of a Stokes phenomenon between f_0 and nf_2 or even between f_1 and nf_2, but these are of lower exponential order and will not concern us here.

It is important now to recall that $x = x_{c+}$ is not a turning point/caustic for 0 and nf_1. At $x = x_{c+}$, $nf_1 \neq 0$, and so the $a_r^{(0)}$ are well-behaved and possess no singularities. Hence the activity of the Stokes curve $S_{0>1}$ has changed at a perfectly regular point. Why has this happened? It is because of the presence of the higher-order Stokes curve that passes through $x = x_{c+}$ on the Stokes curve $S_{0>1}$ (see figure 4). The higher-order Stokes curve has switched off the Stokes curve $S_{0>1}$ at this regular point [5, 6, 10].

If we continue along the line $S_{0>1}$ in the negative-x-direction the singularities nf_1 all move towards f_0 in the Borel plane, see x_H. At the point (x_S, t) the nf_1 appear to coalesce with f_0, and so from the point of view of the Borel plane, this point is apparently a caustic/turning point of the asymptotics. If this were a true turning point the derivatives in individual terms in the asymptotics would diverge at x_S. An examination of the coefficients $a_r(x, t)$ shows that this is not the case. The reason for this is that, as suggested above, all the singularities nf_1 and 0 *indeed do lie on mutually different Riemann sheets*: this is only an apparent coalescence. In the notation of [1], this is a *virtual turning point*. (Note that the definition of a virtual turning point in [10] did not coincide with that of [1], with which we henceforth comply.)

Now we can make a set of key remarks:

- The terms in the transseries do not diverge at x_S. This is because x_S is only a virtual turning point, since the relevant apparently coalescing Borel singularities are, in fact, on distinct Riemann sheets. Hence the Borel singularities have accumulated to create a smoothed shock rather than a caustic.
- The reason that the Borel singularities are on distinct sheets is the presence of the higher-order Stokes curve. This sprouts from the real caustics either side of the shock and separates x_S from the region of space outside the turning points.
- Without the higher-order Stokes curve, the Riemann-sheet structure of the Borel plane would remain unchanged along the path $x_A \to x_B \to \cdots \to x_G \to x_S$. In that event, nf_1 singularities would coalesce on the same Riemann sheet at the shock point, x_S, resulting in the divergence of individual terms in the asymptotics. Hence, the analytic continuation of the asymptotics from the outside to the inside of the shock region, around $x > x_{c+}$, would result in a caustic and not a shock at x_S. Therefore, if it were not for the higher-order Stokes phenomenon, the shock would be a caustic. Hence, when viewed from the standpoint of exponential asymptotics, the higher-order Stokes phenomenon is an essential part of the mechanism for forming the smoothed (propagating) shock.
- Note that there is an anti-Stokes curve passing through the shock position along which $\Re f_1 = 0$. It is well known that on or close to such lines exact solutions may indeed blow up. This is reflected in the summed transseries represention by the presence of poles when $\mathrm{e}^{-f_1/\epsilon} = \mathcal{O}(1)$. Specifically, the second term in (45) has poles where

$$f_1 = -\epsilon \left((2p+1)\pi \mathrm{i} + \ln \left(\frac{K_{01} a_0^{(1)}}{2(\partial f_1/\partial x)} \right) \right), \qquad p \in \mathbb{Z}. \tag{91}$$

  The presence of anti-Stokes curves in nonlinear problems generating such singularities would usually present a difficulty to further analytic continuation of asymptotic solutions to regions $x < x_S$. However, here we can still proceed by continuing precisely the shock point using the summed approximation (45). For an analogous discussion in the context of nonlinear ordinary differential equations see [7].

- In section 5.2 we have determined $a_0^{(1,1)}$ in such a way as to show that the Stokes multiplier $K_{01} = 1$. Note that we have not determined the coefficients $a_r^{(1,1)}$, $r \geqslant 1$. These coefficients satisfy a recurrence relation that is an inhomogeneous version of (30). Hence, associated with all these coefficients would be 'constants of integration' that would have to be determined. We have not determined these coefficients, since the main purpose of this paper is to show how exponential asymptotics lead to the smoothed shock. However, were we to try to determine these extra coefficients, then we might encounter the problem that there is no natural point in the (x, t) plane at which to anchor them and thus set their integration constants. In [17] it is illustrated how such a phenomenon can lead to ϵ dependence within the Stokes multipliers.

In figure 5 we plot the complex x-plane for $t = 1/4 < t_c$ and $t = 5 > t_c$ for $\epsilon = 0.075$. The Stokes lines and higher-order Stokes lines are shown. In each region separated by Stokes lines the contributing transseries are denoted by indices in brackets. For example (0, 1) means that f_0 and a transseries involving f_1 contributes to the asymptotics.

The positions of the viscous poles are shown as dots in the complex region surrounding the shock. The union of all such sections would generate Stokes, anti-Stokes and higher-order Stokes surfaces between the caustics.

When $t = 1/4 < t_c$ higher-order Stokes lines sprout from the caustics $\mathcal{C}_{01}$ and $\mathcal{C}_{02}$. As $t \to t_c$ the region enclosed by these lines shrinks to nothing when $\mathcal{C}_{01}$ and $\mathcal{C}_{02}$ coalesce, but then grows again, pinned to the $\mathcal{C}_R$ as can be seen in the plot for $t = 5 > t_c$.

For $t < t_c$, the $\mathcal{C}_{01}$ and $\mathcal{C}_{02}$ are joined by an irrelevant Stokes line [10]. Along this line the term contributing to the asymptotics comes from the singularity at f_0, which is itself subdominant to both f_1 and f_2. However since contributions from neither f_1 nor f_2 are present, they cannot switch off the contribution from f_0. Hence as one crosses this line, there is no change in the asymptotics.

Finally, we briefly examine the analytic behaviour of the solution deep into the complex-x plane and removed from the region surrounding the shock. Without loss of generality, we consider the upper half plane $\Im(x) > 0$.

Consider the Stokes curve $S_{0>1}$ from $\mathcal{C}_{01}$ to $\mathcal{C}_{01'}$. At $\mathcal{C}_{01}$ f_1 coalesces with 0. At $\mathcal{C}_{01'}$, f_1' $(= f_1 - \pi/2)$ coalesces with 0. As one move along $S_{0>1}$, we have Re $f_{1'} > 0 >$ Re f_1. This is actually a double Stokes line $S_{0>1}$ and $S_{1'>0}$ (as found in the WKB treatment of quantum barrier scattering problems) but the latter is irrelevant since $f_{1'}$ is not contributing in this region.

As can be checked by breaking the symmetry by giving ϵ a small imaginary part, a double Stokes line also sprouts from $\mathcal{C}_{01'}$ separating Stokes regions where 0, f_1 and 0, $f_{1'}$ contribute. We have denoted this by $S_{0>1'} \cup S_{0>1}$. Along this line $0 >$ Re $f_{1'} >$ Re f_1. Thus 0 switches on f_1' as the line is crossed in the anticlockwise sense. Simultaneously, however, 0 switches off a contribution from f_1.

Further viscous poles are also found near to anti-Stokes lines emerging from $\mathcal{C}_{0j'}$, $j = 1, 2$ within the region bounded by two Stokes lines $S_{0>1'}$. These poles are found in the resummation of the transseries arising from the contribution from f_1' as the Stokes line $S_{0>1'}$ are crossed; see also appendix B.

A similar argument applies to the region surrounding $\mathcal{C}_{02'}$.

7. Conclusions

We have demonstrated how an exponential-asymptotic approach can be used to model the formation of a smoothed shock wave arising in a PDE system through the resummation of transseries. The exponential-asymptotic result naturally accounts for and incorporates the

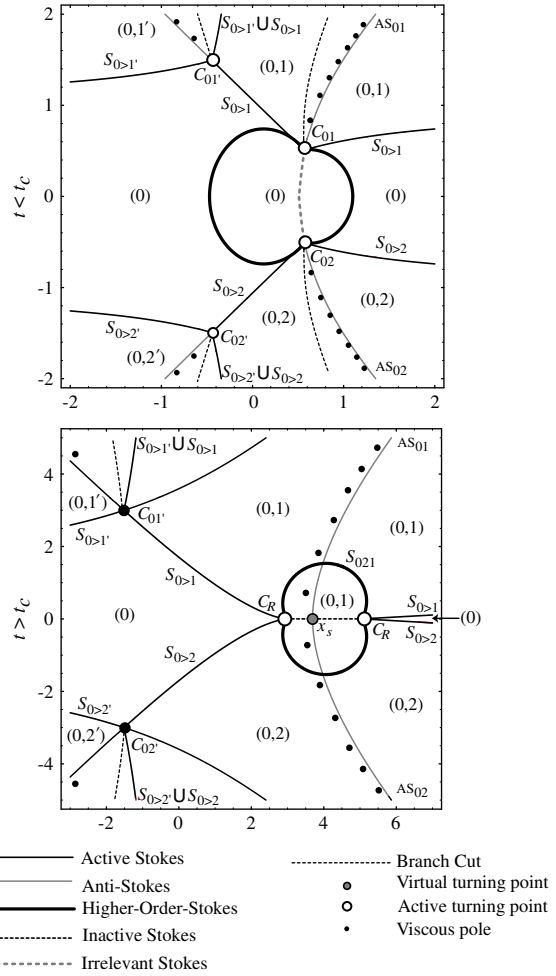

Figure 5. Location of the Stokes, anti-Stokes and higher-order Stokes lines, together with the complex poles, caustics and shock location x_s (a virtual caustic) in the complex x-plane surrounding the shock region for $t = 1/4 < t_c$ (left) and $t = 5 > t_c$ (right), both for $\epsilon = 0.075$. The numbers in brackets within a Stokes region, denote the family of Borel singularities that are contributing to the asymptotics. For example, (0, 1) means that f_0 and nf_1, $n = 1, 2, 3\cdots$ are all switched on. As ϵ decreases towards zero, the density of the poles along the relevant anti-Stokes lines increases. Note that we have here aligned the branch cuts for convenience of discussion; the viscous problem unambiguously instead selects these to lie along the anti-Stokes lines, these being the lines along which the inviscid limit of the viscous solution changes identity.

location of the smoothed shock without the explicit need for a Rankine–Hugoniot condition. The exponential asymptotics extend the range of validity of matched asymptotics.

We have hence shown that the higher-order Stokes phenomenon plays a significant role in the analytical properties of the solution of a nonlinear PDE system that forms a smoothed shock wave. Without the presence of the higher-order Stokes phenomenon the shock wave would have evolved into a caustic of the asymptotic expansion. Conversely the avoidance of a caustic at the smoothed shock wave can be regarded as indicative of the presence of a higher-order Stokes phenomenon.

The approach we have taken here does not rely on the specific details of the example we have chosen and so can be generalized to other nonlinear PDE systems. An indication of the general approach to the summation of transseries arising in PDE systems can be found in [9]. This will be expanded on elsewhere.

Hence the higher-order Stokes phenomenon can be expected to play a generic role in the asymptotic properties of smoothed shock formation arising in nonlinear PDEs.

Acknowledgments

This work was supported by the EPSRC Grant GR/R18642/01 and was initiated during a meeting at Woolsthorpe Manor. Two of the authors (CJH and AOD) acknowledge the generous hospitality of the Research Institute for Mathematical Sciences (University of Kyoto) and the Centrum voor Wiskunde en Informatica (Amsterdam) during phases of this work.

Appendix A. Borel transform representation and Borel-singularity analysis

In this appendix we briefly introduce some fundamental concepts of exponential asymptotics, the Borel transform and the Borel plane. Further details can be found in [15, 16]. We also discuss the detailed Borel-plane singularity structure of the problem under consideration.

First, we define the 'Borel transform' of the solution $u^{(0)}(x,t;\epsilon)$ to be the Taylor series

$$y^{(0)}(x,t;\tau) = \sum_{r=0}^{\infty} \frac{a_r(x,t)}{r!}\tau^r. \tag{A.1}$$

This series converges for $|\tau| < \min\left(|f_1(x,t)|, |f_2(x,t)|\right)$. The connection between $u^{(0)}(x,t;\epsilon)$ and $y^{(0)}(x,t;\tau)$ is the Laplace transform

$$u^{(0)}(x,t;\epsilon) = \epsilon^{-1}\int_0^{\infty} \mathrm{e}^{-\tau/\epsilon} y^{(0)}(x,t;\tau)\,\mathrm{d}\tau. \tag{A.2}$$

This integral representation holds for real (x,t) outside the real caustics.

Note that for the integral in (A-2) to be well-defined one has to show that there exists a real-valued function $K(x,t)$ such that $\left|y^{(0)}(x,t;\tau)\right| \leqslant \exp(K(x,t)|\tau|)$ for large $|\tau|$. This can be done either by obtaining bounds for the coefficients $a_r(x,t)$ or by using the equation

$$y_t^{(0)}(x,t;\tau) + a_0(x,t)y_x^{(0)}(x,t;\tau) + \int_0^{\tau} y_x^{(0)}(x,t;\tilde{\tau})y_{\tau}^{(0)}(x,t;\tau-\tilde{\tau})\,\mathrm{d}\tilde{\tau} = \int_0^{\tau} y_{xx}^{(0)}(x,t;\tilde{\tau})\,\mathrm{d}\tilde{\tau}.$$

We omit the lengthy details.

The complex τ plane is called the 'Borel plane'. To obtain a full understanding of the exponential asymptotics, and to appreciate fully the subtleties of the formation of the shock wave, we need to study the Riemann-sheet structure of this Borel plane.

In section 4 we obtained (33) as the full asymptotic expansion. We deduce that the Borel transform has branch points at $\tau = nf_j$, $j = 1, 2$, $n = 1, 2, 3, \ldots$. That is, seen from the origin, where $y^{(0)}(x,t;\tau)$ is defined, there is a branch point at $\tau = nf_j$. The singular behaviour of $y^{(0)}(x,t;\tau)$ at this branch point is

$$(2\pi i)^{-1}\ln\left(\tau - nf_j(x,t)\right)y^{(n,j)}(x,t;\tau), \tag{A.3}$$

where the $y^{(n,j)}(x,t;\tau)$ are the Borel transforms of $u^{(n,j)}(x,t;\epsilon)$. These functions are defined via the Taylor-series expansions

$$y^{(n,j)}(x,t;\tau) = \sum_{r=0}^{\infty} \frac{a_r^{(n,j)}(x,t)}{r!}\left(\tau - nf_j(x,t)\right)^r. \tag{A.4}$$

From the definition (A.4), the series $y^{(1,1)}(x,t;\tau)$ and $y^{(1,2)}(x,t;\tau)$ are expansions about the points $\tau = f_1$ and $\tau = f_2$, respectively.

We now show that $y^{(1,1)}(x,t;\tau)$ has a branch point at $\tau = f_2(x,t)$. This result follows from the fact that $u^{(1,1)}(x,t;\epsilon)$ and $u^{(1,2)}(x,t;\epsilon)$ are both solutions of the linear homogeneous equation (27), and that $f_1(x,t)$ and $f_2(x,t)$ coalesce at the real caustics $\mathcal{C}_R$. The coalescence gives rise to branch-cut behaviour in the asymptotic expansions of $u^{(1,j)}(x,t;\epsilon)$ at the caustic. However, the solutions of (27) are analytic in x and t near the caustic. Thus the optimal number of terms [14] in the asymptotic expansions of $u^{(1,j)}(x,t;\epsilon)$ must go to zero when we approach the real caustic. Since the optimal number of terms is related to the distance of the point of expansion of the Borel transform from its nearest singularity on the same Riemann sheet, it follows that $y^{(1,1)}(x,t;\tau)$ must have a branch point at $\tau = f_2(x,t)$. Likewise $y^{(1,2)}(x,t;\tau)$ must have a branch point at $\tau = f_1(x,t)$.

In [15, 16] it is explained how the other singularities in the Borel plane can be obtained by formal substitution of transseries into (27). As we have seen in the previous paragraph, the exponential behaviour of the solutions of (27) are $\exp(-f_1/\epsilon)$ and $\exp(-f_2/\epsilon)$. The transseries expansion of the $u^{(0)}(x,t;\epsilon)$ in (27) is the right-hand side of (33). When we formally substitute corresponding transseries expansions for $u^{(1)}(x,t;\epsilon)$ in (27) we see that, to obtain a balance at all orders, the exponentials in these transseries must be of the form $\exp(-(f_j + mf_k)/\epsilon)$, where j and k are either 1 or 2 in value. A transseries of this form is only *permissible* [15, 16] for $u^{(1,1)}(x,t;\epsilon)$ when there exists a phase of ϵ such that $\Re\,(f_1/\epsilon)$, $\Re\,((f_j + mf_k)/\epsilon)$, $m = 1, 2, 3, \ldots$ is an increasing sequence. Hence, the possible locations of branch points for the Borel transform $y^{(1,1)}(x,t;\tau)$ are

$$\tau = (m+1)f_1(x,t), \qquad \tau = f_1(x,t) + mf_2(x,t),$$
$$\tau = mf_2(x,t), \qquad \tau = f_2(x,t) + mf_1(x,t),$$

for $m = 1, 2, 3, \ldots$. The visibility from $\tau = f_1(x,t)$ of these moveable singularities will change as we vary (x,t). This is illustrated in section 6. However, the singularity at $\tau = f_2(x,t)$ is always visible from $\tau = f_1(x,t)$. Note that in general $y^{(1,1)}(x,t;\tau)$ has no singularity at $\tau = 0$.

Since the singularity of $y^{(1,1)}(x,t;\tau)$ at $\tau = f_2(x,t)$ is always visible from $\tau = f_1(x,t)$, as we approach the caustic $\mathcal{C}_R$, (where $f_1 = f_2$) the radius of convergence in (A.4) goes to zero and the corresponding asymptotic coefficients blow up.

According to (A.5) $y^{(1,1)}(x,t;\tau)$ might also see a singularity at $\tau = 2f_2(x,t)$. The question then arises as to whether the set of points where $f_1 = 2f_2$ is also a caustic. When $|2f_2 - f_1| < |f_2 - f_1|$, the sequence $f_1, f_2, 2f_2, 3f_2, \ldots$ does not correspond to a permissible transseries. Hence, for those points $y^{(1,1)}(x,t;\tau)$ does not have singularity at $\tau = 2f_2(x,t)$ and so no caustic can exist.

In a similar way, we can determine from (28) all the visible singularities of $y^{(n,j)}(x,t;\tau)$ for $n > 1$. The possible locations of branch points for the Borel transform $y^{(n,1)}(x,t;\tau)$ are

$$\tau = (m+n)f_1(x,t), \quad \tau = nf_1(x,t) + mf_2(x,t), \qquad m = 1, 2, 3, \ldots. \tag{A.5}$$

Likewise, the possible locations of branch points for the Borel transform $y^{(n,2)}(x,t;\tau)$ are

$$\tau = (m+n)f_2(x,t), \quad \tau = nf_2(x,t) + mf_1(x,t), \qquad m = 1, 2, 3, \cdots. \tag{A.6}$$

The visibility of these singularities will again vary with (x,t). The reason that there are more possible singularities in (A.5) is that the final two arrays of possible singularities in (A.5) are a consequence of the homogeneity of (27), which allows for more transseries solutions.

The locations of singularities visible from $\tau = f_0(x,t)$, $\tau = f_1(x,t)$ and $\tau = nf_1(x,t)$ are indicated in figure 6 for a typical value of (x,t) upstream of the shock. Note that for certain

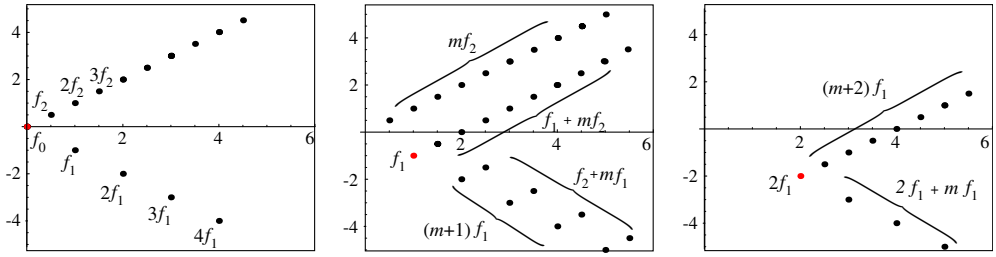

Figure 6. The locations of singularities visible in the Borel plane from 0 (left), f_1 (A.5) (middle) and $2f_1$ (A.5) with $n = 2$ (right) for a typical value of (x_A, t) outside the caustic. In each picture $m = 1, 2, 3\ldots$: see text for explanation.

values of (x, t) these singularities may appear to coalesce in the Borel plane. However, only when the singularities lie on the same Riemann sheet can this give rise to actual caustics. This observation underpins the results of the main text.

Appendix B. Complex-plane-singularity structure

In this appendix we gather together, for ease of reference, some pertinent general results on the singularity structure of both the inviscid ($\epsilon = 0$) and viscous problems, and then discuss the small, near-shock-formation and large-time behaviour of the current problem. This work is independent of the derivations of the main paper.

For the inviscid problem, a branch point in the leading-order solution is located at

$$X = S(t), \qquad x = s(t) = S(t) + F(S)t, \qquad F'(S(t)) = -1/t \tag{B.1}$$

in which the initial data is $u(x, 0) = a_0(x, 0) = F(x)$ and the final equation in (B.1) determines possible locations $s(t)$. It is then readily shown (perhaps using the results that $\dot{s} = F(S), \ddot{s} = -1/\left[t^3 F''(S)\right]$) that

$$a_0 \sim \dot{s} \pm \sqrt{-2\ddot{s}(x - s)} \qquad \text{as } x \to s. \tag{B.2}$$

where the dot denotes differentiation with respect to t. Such square-root branch cuts represent the generic form of a singularity of a_0.

The expression (B.2) implies that the appropriate inner scalings which bring in the viscous term in (1) are

$$x = s(t) + \epsilon^{2/3} z, \qquad u = \dot{s}(t) + \epsilon^{1/3} v \tag{B.3}$$

whereby

$$\ddot{s} + \epsilon^{1/3} \frac{\partial v}{\partial t} + v \frac{\partial v}{\partial z} = \frac{\partial^2 v}{\partial z^2} \tag{B.4}$$

so, up to a translation in z (which could be absorbed by a redefinition of $s(t)$) at leading order we obtain the Riccati equation

$$\ddot{s} z + \frac{1}{2} v_0^2 = \frac{\partial v_0}{\partial z} \tag{B.5}$$

whose solution, associated with the $\mathcal{C}_{01}$ caustic (see, e.g. figure 5) that matches with (B.2) is given by

$$v_0 = -(-4\ddot{s})^{1/3} \mathrm{Ai}'\left((-\ddot{s}/2)^{1/3} z\right) / \mathrm{Ai}\left((-\ddot{s}/2)^{1/3} z\right). \tag{B.6}$$

The expression (B.6) illustrates the accumulation of poles in the viscous problem that occurs in the neighbourhood of the invisicid singularities; these are arrayed for large $|z|$ along the anti-Stokes line of $\mathrm{Ai}(\zeta)$ (i.e. along $\arg\zeta = \pm\pi$), a phenomenon that extends along the anti-Stokes line into the outer region. The local form of the viscous solution at a pole $x = \sigma(t)$ is given by the quasi-steady balance

$$u \sim -2\epsilon/(x - \sigma(t)), \tag{B.7}$$

which gives no information about pole dynamics (though these can be constructed by other means, see, e.g. [3]).

For the specific initial data $F(x) = 1/(1+x^2)$ discussed above we can derive the small-time behaviour of (B.1) in the form

$$S \sim \mathrm{e}^{\pm\mathrm{i}\pi/2} \pm \mathrm{e}^{\mp\mathrm{i}\pi/4}\sqrt{t/2}, \qquad s \sim \mathrm{e}^{\pm\mathrm{i}\pi/2} \pm \mathrm{e}^{\mp\mathrm{i}\pi/4}\sqrt{2t}, \qquad \text{as } t \to 0, \tag{B.8}$$

where the upper and lower signs within the exponentials go together but are independent of those that are not exponentiated. Thus in the upper half plane, say, one invisicid singularity moves in $\Re(x) > 0$ towards the real axis, while the other moves away in $\Re(x) < 0$. The initial data we have chosen shares the simple-pole structure (B.7) of the viscous problem, though the coefficient is different. This coincidence leads to the small-time viscous behaviour being addressed most concisely by taking the limits in the 'opposite' order, i.e. the ϵ term is retained in (1) and the limit $t \to 0$ is taken, via the similarity reduction

$$u \sim t^{-1/2}\Phi\left(\frac{x - i}{t^{1/2}}\right) \qquad \text{as } t \to 0^+, \ |x - i| \ll 1, \tag{B.9}$$

which yields at leading order in t the Riccati equation

$$-\frac{i}{4} - \frac{1}{2}\eta\Phi + \frac{1}{2}\Phi^2 = \epsilon\frac{\mathrm{d}\Phi}{\mathrm{d}\eta} \tag{B.10}$$

for $\Phi(\eta;\epsilon)$, which tends to $-i\eta/2$ as $\eta \to \infty$. Setting

$$\Phi = -\frac{2\epsilon}{\Psi}\frac{\mathrm{d}\Psi}{\mathrm{d}\eta} \tag{B.11}$$

furnishes the equation

$$\frac{\mathrm{d}^2\Psi}{\mathrm{d}\eta^2} + \frac{\eta}{2\epsilon}\frac{\mathrm{d}\Psi}{\mathrm{d}\eta} - \frac{i}{8\epsilon^2}\Psi = 0 \tag{B.12}$$

whose solution can be expressed in terms of parabolic cylinder functions.

The ODE (B.12) has a surprisingly delicate exponential-asymptotic structure, namely much of that illustrated in the upper picture in figure 5, which arises from turning points at $\eta = \pm\mathrm{e}^{-\mathrm{i}\pi/4}\sqrt{2}$ (cf (B.8)).

The second limit (i.e. other than $t \to 0^+$) in which the singularity structure becomes more involved is near the time of shock formation. At this time the (arrays of viscous singularities associated with the) inviscid singularities in $\Im(x) > 0$ and $\Im(x) < 0$ collide on the real axis (i.e. $\mathcal{C}_{01}$ and $\mathcal{C}_{02}$ in figure 5, each of which carries a trail of viscous singularities in its wake, collide). Taking the time, location and height of shock formation to be, respectively, $t = t^*$, $x = x^*$ and $u = u^*$, the appropriate rescalings are

$$t = t^* + \epsilon^{1/2}\tau, \qquad x = x^* + \epsilon^{1/2}u^*\tau + \epsilon^{3/4}y, \qquad u = u^* + \epsilon^{1/4}w, \tag{B.13}$$

(leading-order expressions for these can be deduced from the inviscid solution, whereby X^* is given by $F''(X^*) = 0$ and then

$$t^* = -1/F'(X^*), \qquad x^* = X^* + F(X^*)t^*, \qquad u^* = F(X^*); \tag{B.14}$$

moreover, at $t = t^*$ the inviscid solution then has a profile

$$u - u^* \sim -\left(6(x - x^*)/\left[F'''(X^*)t^{*4}\right]\right)^{1/3} \qquad \text{as } x \to x^*, \tag{B.15}$$

with $F'''(X^*)$ non-negative and generically positive, which henceforth we assume) giving the full balance

$$\frac{\partial w}{\partial \tau} + w\frac{\partial w}{\partial y} = \frac{\partial^2 w}{\partial y^2}. \tag{B.16}$$

The leading-order problem then involves the initial data

$$w_0 \sim (-\tau)^{1/2}\Lambda\left(y/(-\tau)^{3/2}\right) \qquad \text{as } \tau \to -\infty \tag{B.17}$$

where $\Lambda(\xi)$ is a similarity solution to the inviscid problem, being given by

$$\alpha\Lambda^3 + \Lambda + \xi = 0, \tag{B.18}$$

where (B.15) gives $\alpha = F'''(X^*)(t^*)^4/6$; (B.18) identifies the inviscid singularities as having asymptotic behaviour $y \sim \pm 2i(-\tau)^{3/2}/3\sqrt{3\alpha}$ as they approach the real axis. The initial value problem for w_0 can be solved by the Cole–Hopf transformation (say; the result is perhaps most readily derived by inserting the scalings associated with (B.13) into the exact solution to the initial value problem with $u = F(X)$ at $t = 0$ and re-expanding—the calculation is in any case rather delicate) in the form

$$w_0(y,\tau) = -\frac{1}{t^*}\frac{\int_{-\infty}^{+\infty}\rho\exp\left(-\dfrac{F'''(X^*)}{48}\rho^4 + \dfrac{\tau\rho^2}{4(t^*)^2} + \dfrac{y\rho}{2t^*}\right)}{\int_{-\infty}^{+\infty}\exp\left(-\dfrac{F'''(X^*)}{48}\rho^4 + \dfrac{\tau\rho^2}{4(t^*)^2} + \dfrac{y\rho}{2t^*}\right)}, \tag{B.19}$$

a saddle-point estimate of this integral reproducing (B.18). We note that (B.19) is proportional to the logarithmic derivative of a complex Pearcey function with respect to y.

Finally, the large-time behaviour also warrants discussion. The appropriate scalings are

$$x = X/\epsilon, \qquad t = T/\epsilon^3, \qquad u = \epsilon^2 U \tag{B.20}$$

to yield at leading order the initial value problem

$$\frac{\partial U_0}{\partial T} + U_0\frac{\partial U_0}{\partial X} = \frac{\partial^2 U_0}{\partial X^2}, \qquad \text{as } T \to 0^+ \quad U_0 \sim T^{-2/3}\Xi\left(X/T^{1/3}\right), \tag{B.21}$$

where $\Xi(Z)$ is the inviscid similarity solution

$$Z = -\Xi^{-1/2} + \Xi, \tag{B.22}$$

a form that follows from consideration of how the initial data for u transforms.

This problem has explicit solution

$$U_0 = \frac{1}{T}\frac{\int_{-\infty}^{0}(X - X')\exp\left(-\dfrac{(X-X')^2}{4T} + \dfrac{1}{2X'}\right)\mathrm{d}X'}{\int_{-\infty}^{0}\exp\left(-\dfrac{(X-X')^2}{4T} + \dfrac{1}{2X'}\right)\mathrm{d}X'}, \tag{B.23}$$

whose denominator can be expressed in the form

$$\int_{-\infty}^{0}\exp\left(-\frac{(X-X')^2}{4T} + \frac{1}{2X'}\right)\mathrm{d}X' = 2\sqrt{T}\mathrm{e}^{-X^2/4/T}\sum_{n=0}^{\infty}\left(-\frac{1}{4}\right)^n\frac{K_{2n+1}(\sqrt{X/T})}{n!X^{n+1/2}}.$$

The expression evolves for large time to the familiar similarity solution

$$U_0 \sim T^{-1/2}\hat{\Xi}\left(\hat{Z}\right), \qquad \hat{Z} = X/T^{1/2} \quad \text{as} \quad T \to \infty, \tag{B.24}$$

with $\hat{\Xi}$ readily obtained directed in the form

$$\hat{\Xi}\left(\hat{Z}x\right) = \frac{2\mathrm{e}^{-\hat{Z}^2/4}}{\sqrt{\pi}\ \mathrm{erfc}\left(\hat{Z}/2\right)} \tag{B.25}$$

whose poles lie in the far field $|\hat{Z}| \to \infty$ along the rays $\arg \hat{Z} = \pm 3\pi/4$. We remark from (B.22) that the inviscid branch points associated with the intermediate timescale (i.e. $t \gg 1$ with $T \ll 1$) correspond to the $\mathcal{C}_{01'}$ and $\mathcal{C}_{02'}$ singularities in figure 5. The poles of (B.25) provide the ultimate fate of the associated trails of viscous singularities along the left-hand anti-Stokes lines and in this limit satisfy

$$x \sim \frac{3}{2^{2/3}}\mathrm{e}^{\pm 2\pi \mathrm{i}/3} t^{1/3}. \tag{B.26}$$

References

[1] Aoki T, Kawai T and Takei Y 2001 On the exact steepest descent method: a new method for the description of Stokes curves *J. Math. Phys.* **42** 3691–713

[2] Berry M V and Howls C J 1990 Stokes surfaces of diffraction catastrophes with co-dimension three *Nonlinearity* **3** 281–90

[3] Bessis D and Fournier J D 1984 Pole condensation and the Riemann surface associated with a shock in Burgers' equation *J. Physique Lett.* **45** L833–41

[4] Bessis D and Fournier J D 1990 Complex singularities and the Riemann surface for the Burgers equation *Proc. Int. Conf. Research Reports in Physics—Nonlinear (Shanghai, China)* (Berlin: Springer)

[5] Body G L, King J R and Tew R H 2005 Exponential asymptotics of a fifth-order partial differential equation *Eur. J. Appl. Math.* **16** 647–81

[6] Chapman S J and Mortimer D M 2005 Exponential asymptotics and Stokes line in a partial differential equation *Proc. R. Soc. Lond. Ser. A: Math. Phys. Eng. Sci.* **461** 385–2421

[7] Costin O and Costin R D 2001 On the formation of singularities of solutions of nonlinear differential systems in antistokes directions *Invent. Math.* **145** 425–85

[8] Dingle R B 1973 *Asymptotic Expansions: Their Derivation and Interpretation* (New York: Academic)

[9] Howls C J 2007 On the use of Z-transforms in the summation of transerries for partial differential equations *R.I.M.S. Kokyuroku, 'Algebraic Analysis of Differential Equations'* (Japan: University of Kyoto) submitted

[10] Howls C J, Langman P J and Olde Daalhuis A B 2004 On the higher order Stokes phenomenon *Proc. R. Soc. Lond. Ser. A: Math. Phys. Eng. Sci.* **460** 2285–303

[11] Howls C J and Olde Daalhuis A B in preparation

[12] Groen P P N and Karadzhov G E 1998 Exponentially slow travelling waves on a finite interval for Burgers' type equation *Electron. J. Diff. Eqns* **30** 1–38

[13] Langman P J 2005 *PhD Thesis* University of Southampton

[14] Olde Daalhuis A B 1998 Hyperasymptotic solutions of highter order linear differential equations with a singularity of rank one *Proc. R. Soc. Lond. Ser. A: Math. Phys. Eng. Sci.* **454** 1–29

[15] Olde Daalhuis A B 2005 Hyperasymptotics for nonlinear ODEs I: A Riccati equation *Proc. R. Soc. Lond. Ser. A: Math. Phys. Eng. Sci.* **461** 2503–20

[16] Olde Daalhuis A B 2005 Hyperasymptotics for nonlinear ODEs: II. The first Painlevé equation and a second order Ricatti equation *Proc. R. Soc. Lond. Ser. A: Math. Phys. Eng. Sci.* **461** 3005–021

[17] Ólafsdóttir E I, Olde Daalhuis A B and Vanneste J 2005 Stokes-multiplier expansion in an inhomogeneous differential equation with a small parameter *Proc. R. Soc. Lond. Ser. A: Math. Phys. Eng. Sci.* **461** 2243–56

[18] Senouf D 1997 Dynamics and condensation of complex singularities for Burgers' equation *SIAM J. Math. Anal.* **28** 1457–89

[19] Senouf D 1997 Dynamics and condensation of complex singularities for Burgers' equation *SIAM J. Math. Anal.* **28** 1490–513

[20] Ward M J 1998 Exponential asymptotics and convection–diffusion–reaction models *Analyzing Multiscale Phenomena Using Singular Perturbation Methods*, *Proc. Symp. in Applied Mathematics* vol 56 (Philadelphia, PA: SIAM) pp 151–84

[21] Whitham G B 1974 *Linear and Nonlinear Waves* (New York: Wiley-Interscience)